VILNIUS UNIVERSITY

FACULTY OF CHEMISTRY AND GEOSCIENCES

GEOLOGY

Anar Bakhtiyarov

MASTER THESIS

RESEARCH OF OEDOMETRIC MODULUS AND ITS CORRELATION WITH CONE PENETRATION TEST RESULTS IN OVERCONSOLIDATED PLEISTOCENE FINE-GRAINED TILL SOILS

PERTANKINTŲ PLEISTOCENO MORENINIŲ SMULKIŲ GRUNTŲ OEDOMETRINIO DEFORMACIJŲ MODULIO TYRIMAI IR KORELIACIJA SU STATINIO ZONDAVIMO DUOMENIMIS

Supervisor: Gintaras Žaržojus

Vilnius, 2024

TABLE OF CONTENTS

ABSTRACT

This thesis investigates the relationship between the oedometric modulus (Eoed) and cone tip resistance (qc) in overconsolidated Pleistocene fine-grained till soils. Utilizing data from multiple Kelmė soil samples, correlation and regression analyses were conducted under varying stress levels using different analytical tools and EViews software.

The findings reveal predominantly weak and statistically insignificant relationships between qc and Eoed. For Kelmė 19-1, a moderate negative correlation was identified, but regression analyses indicated that this relationship was not statistically significant. Kelmė 19-2 exhibited weak positive correlations, with both linear and polynomial regression models failing to achieve statistical significance. Similarly, Kelmė 37-2 demonstrated weak correlations and low explanatory power, suggesting no meaningful relationship between qc and Eoed.

Specific stress analyses further supported these conclusions. Under 39 kPa stress, a moderate direct relationship was observed, yet the regression model lacked statistical significance and explanatory power. At 625 kPa stress, a weak inverse relationship was detected, but the regression model again did not significantly explain the variability in Eoed.

Overall, the study highlights the complexity of predicting Eoed from qc in overconsolidated Pleistocene fine-grained till soils. The research underscores the limitations of laboratory tests in replicating real-world conditions and calls for further studies with more comprehensive models to better understand soil behaviour. These insights are critical for geotechnical engineering applications, offering a nuanced understanding of soil properties and their interactions.

Key words: Correlation, overconsolidated Pleistocene fine-grained till soils, oedometric modulus, cone penetration test, regression analysis

INTRODUCTION

Moraine (till) soils are landforms that are typically found in areas previously covered by glaciers or ice sheets. They are composed of glacial debris, including rocks, boulders, sand, and clay, that were transported and deposited by the moving ice. Moraines can be found in various parts of the world, including regions that have experienced glaciation in the past, such as North America, Europe, Asia, Siberia and Antarctica. Research on moraine soils is an ongoing and multidisciplinary field. The specific focus and methodologies employed may vary depending on the research objectives and the location of the study area. As these soil types are extremely heterogeneous, this makes their research very challenging and restricted.

The relevance of the topic lies in the fact that this kind of soils (consolidated Pleistocene till soil) has not been explored much and there are very few researches works about it.

The aim of the master thesis is to provide an accurate assessment of the over consolidated Pleistocene till soil oedometric modulus to make correlation with cone penetration test results and provide mathematical validation.

To achieve this goal, it is necessary to solve a number of tasks including the following:

• Introduction of over consolidated fine-grained soils mainly concentrating on moraine deposits;

• Provision of an accurate assessment of the over consolidated Pleistocene till soil oedometric modulus;

• Correlation with cone penetration test results and provision of mathematical validation.

The subject of the master thesis is the accurate assessment of consolidated Pleistocene till soil oedometric modulus. The object of the course work is consolidated Pleistocene fine grained till soils.

Theoretical base of the research: scientific research of domestic and foreign scientists in the field of soils.

Methodological base of the research: comparison, analysis and synthesis, regression analysis. The examination and sample tests are done by using the soil samples of the Kelmé region in Lithuania. Kelmė, located in northwestern Lithuania, is part of the historical region of Samogitia.

I would like to express my sincere gratitude to JSC Geotestus for their invaluable support in providing the soil samples, as well as the comprehensive geotechnical report of the Kelmė district. Their contributions were mandatory to the success of the thesis, and I deeply appreciate their assistance and expertise.

CHAPTER 1

OVERCONSOLIDATED PLEISTOCENE FINE GRAINED TILL SOILS AND CONE PENETRATION TEST

1.1. Introduction to Pleistocene Fine Soils

Moraine till soils, also known as glacial till soils, are a type of soil formed by the deposition of materials carried and deposited by a glacier. Moraine till is a mixture of various sizes of unsorted and unstratified material, including rock fragments, boulders, gravel, sand, silt, and clay. These soils are typically found in regions that have experienced glaciation, where glaciers have transported and deposited sediments (Cepero et al, 2014).

Pleistocene glacial soils, which constitute a substantial portion of Lithuania's landscape, are commonly utilized for diverse applications such as infrastructure, construction, and structural elements (Putys et al., 2010). Despite their widespread use, there remains a notable gap in comprehensive studies addressing the deformation characteristics of these glacial till soils in Lithuania.

The mechanical behaviour of soil and its characteristics exhibit nonlinearity, anisotropy, and elastoplasticity, primarily influenced by variations in soil structure and stress during different loading and unloading conditions (Huang et al., 2018; Li et al., 2022).

Change in stress are recognized as a pivotal factor influencing the deformation characteristics of soil, closely linked to its structure (Li et al., 2022). The settlement or compressibility of soil under self-weight or applied foundation loading highlights the crucial impact of stress paths and consolidation pressure on volume strain (Wei et al., 2023). Soil compressibility results from the reconfiguration of soil grains, contingent upon particle bond strength, skeletal stability, and overall strength. This reconfiguration involves the disruption, rolling, and sliding of soil particles, accompanied by the expulsion or compression of water from voids. Therefore, accurately anticipating the behaviour of time-dependent soil compressibility and its primary determinants is essential (Jayalekshmi, Elamathi, 2020).

One of the vital consolidation characteristics of soil is its compressibility, primarily expressed through the deformation modulus of elasticity (E), defining the elastic region of soil (see Figures 1 and 2) (Sharma et al., 2017; Meyer, Olszewska, 2021). In the numerical Mohr-Coulomb (MC) foundation design model, the Young’s modulus (E') is employed as one of the elastic moduli (refer to Figure 1). The Hardening Soil (HS) model utilizes the oedometer modulus

(E_{oed}) (Gaur & Sahay, 2017; Saleh, 2021). Young's modulus (E') and constrained oedometer deformation modulus (E_{oed}) are interconnected through Poisson's ratio (Lovisa et al., 2015).

Within the Lithuanian context, deformation modulus is understood differently by researchers, engineering geologists, and geotechnicians, being either described by Young's modulus (Figure 1), constrained oedometer deformation modulus (Figure 2), or the general deformation modulus (E_0). The general deformation modulus can be derived from cone penetration test results, considering the correlation coefficient α (Brilingas, 1988). This modulus continues to be utilized, albeit with some adjustments in the correlation coefficient α (EN 1997-2:2007; TAR, 2015-11-16, Nr. 18162).

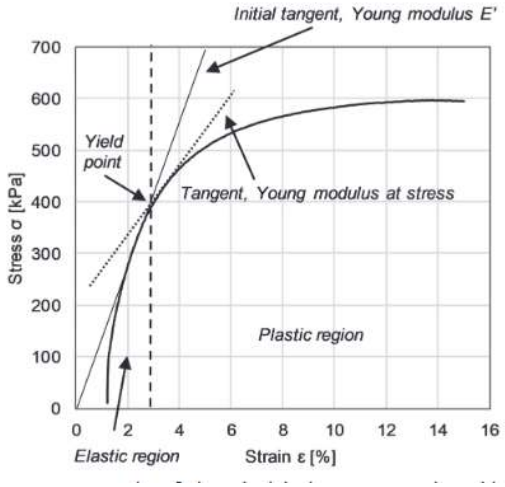

Figure 1: Example of the triaxial shear test results with the identified elastic and plastic zones and the tangent (Young's) modulus (Source: Lekstutytė et al, 2023: 191)

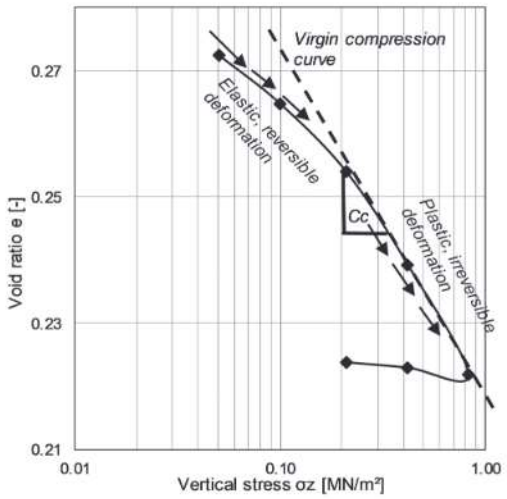

Figure 2: Example of the oedometer compression test results with the identified elastic and plastic zones in the soil consolidation graph (Source: Lekstutytė et al, 2023: 192)

The EN 1997-2:2007 standard plays a significant role as it outlines the formulas and methodology for computing Young's modulus (E') and oedometer deformation modulus (E_{oed}) from cone resistance. It is important to highlight that these formulas are specifically designed for spread foundations and are applicable only under drained conditions. Moreover, the outcomes obtained through these formulas are purely theoretical. In a laboratory setting, the determination of Young's modulus and oedometer deformation modulus can be achieved through the implementation of an oedometer test (according to EN ISO 17892-5:2017) or a triaxial test (as per EN ISO 17892-9:2018). These tests are designed to comprehensively account for all conditions and factors influencing the actual deformation values of the soil (Lekstutytė et al, 2023: 192).

The accurate assessment of soil deformation moduli and, consequently, the overall comprehension of soil deformability and stability are significantly influenced by soil composition. Key factors affecting soil deformation include particle size and the proportion of fine fraction in the soil, both of which contribute to the mechanical properties and stability of the soil. Ultimately, soil deformation and its mechanical characteristics under load are directly impacted by the presence of cracks, layers, and large pores (Wang et al., 2021).

Soil exhibits reduced deformability when its composition includes a smaller proportion of fine fraction, as suggested by Habtemariam et al. (2022). The grain size and distribution within sandy soils play a vital role in determining their deformation characteristics. Sabarishri et al. (2017) found that the deformation modulus tends to increase with the coarsening of the soil fraction.

The quantity and density of natural water content significantly influence soil deformation behaviour and strength. Studies consistently show that an increase in water content leads to a decrease in soil strength, deformation modulus, coefficient of consolidation (Cv), and the angle of internal friction (φ) (Malizia, Shakoor, 2018; Habtemariam et al., 2022). Additionally, clay plasticity affects compressive strength, with some research indicating that compressive strength increases with clay plasticity (Malizia, Shakoor, 2018). However, the impact of medium and high plasticity clays on compressive strength does not exhibit significant differences (Malizia, Shakoor, 2018). These findings emphasize the importance of natural water content and density in understanding soil deformations, consolidation, and their implications for practical soil applications.

De Silvade Silva & Paul (1976) identifies essential key characteristics and properties of moraine till soils as follows. As for them, moraine till soils typically have a loamy texture, which signifies a blend of different particle sizes resulting from glacial movement. The specific makeup of these soils varies depending on the rocks and sediments encountered during the glacial transport

process. The presence of diverse rock types and minerals impacts both the chemical and physical attributes of the soil. Spatial variability is common in moraine till soils due to the uneven deposition of glacial materials. This variability contributes to fluctuations in soil texture. Over-consolidation of soil occurs when it becomes excessively compacted, reducing the size of pore spaces between particles. This compression results in higher soil density and a decreased void ratio. Over-consolidation can affect multiple soil properties, including its strength, stiffness, and settlement characteristics.

Lekstutytė et al. carried out research in 2018 to determine soil properties and investigate the mechanical properties of overconsolidated moraine clay in Medininkai area. The tests were carried out at depths of 6.0 and 20.0 meters. The classification of the tested soil's strength was determined based on the information gathered during the test, specifically the cone resistance (q_c) and sleeve friction (f_s). According to the soil strength classification derived from the cone penetration test, the tested soil is categorized as very strong when the cone resistance exceeds 4 MN/m^2. Examining the outcomes for silt and clay soils, considering the cone resistance (q_c) values, it is essential to apply these results exclusively to drained soils. Upon scrutinizing the values in the literature, it was observed that the suggested shearing strength parameters (Sližytė et al., 2012) tend to be overstated when compared to the obtained results. The literature indicates an internal friction angle that is higher by approximately 5–3° for SCD tests and 6–2° for UCU tests. Moreover, the cohesion values in the literature are elevated by around 54.0–61.0 kPa for SCD tests and 52.0–55.0 kPa for UCU tests. Consequently, significant discrepancies arise, particularly in cohesion (c), which, in certain instances, is up to four times higher. The variations are most pronounced in SCD tests (ranging from 2.9 to 3.9 times higher), while UCU tests exhibit slightly smaller differences (2.6 to 2.9 times higher). Although the differences in the angle of internal friction ϕ° are relatively smaller, varying from 6 to 2°, it is noteworthy that the table is specific to till soil, leading to these disparities. Based on the laboratory results for physical properties, the tested soil is identified as sandy silty clay (till), classified as very strong clays according to field test results.

The degree of over-consolidation is typically quantified using the over-consolidation ratio (OCR), which is the ratio of the maximum past stress experienced by the soil to the current effective stress. Soils with an OCR greater than 1 are considered overconsolidated, while soils with an OCR equal to 1 are normally consolidated (Wu et al, 2021).

1.2. Elastic properties of Pleistocene Over-consolidated Fine-Grained Soils

The Pleistocene over-consolidated fine-grained soils often exhibit complex behaviour due to their geological history, and their elastic properties play a pivotal role in determining their response to external loads and environmental conditions. The study of elastic properties involves the investigation of parameters such as Young's modulus, shear modulus, and Poisson's ratio, which collectively define the soil's ability to deform under stress. These properties not only influence the soil's deformation characteristics but also impact its shear strength, consolidation behaviour, and overall stability. (Fidelibus et al, 2018).

The elastic properties of over-consolidated fine-grained soils can be described using several equations, including:

1. Young's modulus (E) can be defined as the ratio of stress (σ) to strain (ε):

$$E = \sigma/\varepsilon \quad (1)$$

2. Poisson's ratio (υ) is the ratio of lateral strain (ε_l) to axial strain (ε_a) under uniaxial stress:

$$\upsilon = \varepsilon_l/\varepsilon_a \quad (2)$$

3. Shear modulus (G) can be calculated using the following equation:

$$G = E/(2(1 + \upsilon)) \quad (3)$$

4. Bulk modulus (K) can be defined as the ratio of stress (σ) to volumetric strain (ε_v):

$$K = \sigma/\varepsilon_v \quad (4)$$

These equations can be used to model the behaviour of over-consolidated fine-grained soils under various loading conditions, such as uniaxial compression, triaxial compression, or shear. However, it is important to note that these equations may only be applicable within certain ranges of soil parameters and loading conditions, and laboratory testing is often required to determine the actual soil properties.

1.3. Correlation between Oedometric Modulus and Cone resistance

Correlation between Oedometric Modulus and Cone resistance has been carried by a number of researchers (Robertson, 2016; Lekstutytė et al, 2023).

Mohammed et al. (2000) calculated both in situ static cone resistance of different cohesive soils and Young's Modulus by laboratory tests. The following relation has been obtained:

$$E = aq_c^n + bf_c + c\omega_n + d\rho_d + e \quad (5)$$ (Mohammed, 2000)

Here,

E - Young's Modulus,

q_c - the static cone resistance,

f_c – the frictional resistance,

ω_n - the natural water content,

ρ_d - the dry volumetric mass density,

n - an integer (1, 2, 3),

a, b, c, d and e - regression constants.

Empirical relations have also been brought forward between the oedometric deformation modulus (E_{oed}) and the static cone resistance (q_c).

$$E_{oed} = \alpha * q_c \qquad (6)$$ (Mohammed, 2000)

In the course of engineering geological and geotechnical research in Lithuania, for over three decades, the Young's modulus E of soil has been determined using results from Cone Penetration Tests (CPTs) (Žaržojus & Dundulis, 2010). These calculations rely on empirical equations (7) to (10) developed by Brilingas in 1988, which remain in use today in their original form. Brilingas formulated these equations after analysing data from over 250 plate load tests and CPTs conducted to investigate Lithuanian soil conditions. His research focused on glacial, glaciolacustrine, and glaciofluvial deposits from the Upper Pleistocene Nemunas glaciation Baltija glacial stage, all of which are over-consolidated due to glaciation processes. Brilingas's study found a correlation between the cone penetration resistance (q_c) and the Young's modulus (E), with regression equations showing correlation coefficients ranging from 0.75 to 0.84 for fine soils and 0.86 for sands. The empirical equations (7) to (11) used to calculate the Young's modulus based on cone penetration data are detailed separately (Žaržojus et al, 2022: 3).

- glacial loam (till) (gIIIbl):

$$E = 7.4q_c + 7.2 \qquad (7)$$

- glaciolacustrine clay (lgIIIbl):

$$E = 8.1q_c - 3.1 \qquad (8)$$

- glaciolacustrine loam (lgIIIbl):

$$E = 4.8q_c + 4.9 \qquad (9)$$

- glaciofluvial and glacial sands (fIIIbl and gIIIbl):

$$E = 7.8q_c^{0.71} \qquad (10)$$

- generalised linear regression:

$$E = \alpha q_c \qquad (11)$$

In Equation (11), the coefficient α varies according to soil genesis, lithological composition, and cone resistance (q_c) values. For Upper Pleistocene Nemunas glaciation Baltija stage till loam, α ranges from 14 when q_c=1.0 MPa to 8 when q_c=9.0 MPa. For Baltija stage glaciolacustrine loam, α values range from 10 when q_c=1.0 MPa to 5.8 when q_c=5.0 MPa. In clays,

α varies from 5 when q_c=1.0 MPa to 7.5 when q_c=5.0 MPa. For sands, α ranges from 6.5 when q_c=1.0 MPa to 3.3 when q_c=20.0 MPa. When calculating Young's modulus from CPT data using the correlations in Equations (7) to (11), it is mandatory to understand the load range within which the deformation modulus was evaluated. The magnitude of the vertical load is a significant factor in estimating Young's modulus (Tamošiūnas et al., 2020). Since the correlations were derived from the deformation modulus obtained through static plate load tests, it is concluded that the load range limits are between 0.05 MPa and 0.3 MPa (Žaržojus et al, 2022: 6).

Different software programmes like EViews, Phyton are used to do different kinds of correlations in engineering.

CHAPTER 2

LABORATORY TESTS, OEDOMETER TEST AND METHODOLOGY

2.1. Methodology

The study conducted a comprehensive examination and synthesis of databases comprising 10 samples of Pleistocene moraine till soil collected by the author in the Kelmė region of Lithuania. The primary focus was on analyzing the properties of these soil samples. The till soil samples that were tested fall into two categories: low plasticity clay, which has a stiff to hard consistency, and medium plasticity clay, which has a stiff consistency, according to the soil classification system (EN ISO 14688-2:2018). These till soil kinds are considered based on their geotechnical features.

2.2. Consistency Test (Falling Cone Method) ISO 17892-12:2004

The liquid limit test, specifically the falling cone method, is a commonly used soil test in geotechnical engineering to determine the moisture content at which a soil transitions from a liquid to a plastic state. This transition is crucial for assessing the engineering properties and behavior of soils, including their shear strength and consolidation characteristics. The liquid limit test provides valuable information for soil classification, foundation design, and stability analysis (De Silva et al, 2022).

The plastic limit test is a standard laboratory procedure conducted to determine the plastic limit of a soil sample. The plastic limit represents the moisture content at which a soil transitions from a plastic to a semisolid state. This test provides valuable information for geotechnical engineers and soil scientists in characterizing the plasticity and behavior of soils, which is essential for designing foundations, assessing soil stability, and predicting settlement (Duncan et al, 2014).

The Plasticity Index (PI) is an important parameter used in geotechnical engineering to assess the plasticity and clayey nature of soil. It is a measure of the soil's ability to undergo deformation without fracturing and provides insights into its engineering properties (Ibrahim et al, 2012).

The falling cone method is one of the most widely adopted techniques to determine the liquid limit of a soil sample. It involves measuring the moisture content of the soil when it reaches a specific consistency as the cone of a standardized device penetrates the soil surface. The penetration of the cone indicates the point at which the soil ceases to flow and behaves more like a plastic material (Fithri & Solin, 2021).

The plastic limit test involves determining the moisture content at which a soil sample loses its plasticity and becomes too dry to be molded (Jianqiao et al, 2012). This is accomplished by gradually reducing the moisture content of the soil sample until it can no longer be rolled into a thread of specific dimensions without crumbling.

Apparatus:

Cone Penetrometer: The cone penetrometer is a brass cone with a 30° angle and a flat circular base. The cone penetrometer is attached to the carriage assembly and penetrates the soil sample during the test.

Balance: A balance is used to measure the mass of the soil sample and other required components accurately.

Oven: An oven is used to dry the soil sample to determine its moisture content.

Glass plate: A flat glass surface used to work the soil sample.

Mixing dish: A container used to mix the soil sample with water.

Spatula: A tool for mixing and manipulating the soil sample.

Moisture cans: Small, airtight containers to hold soil samples for moisture content determination.

Procedure:

Liquid limit:

- A representative soil sample from a borehole or field site is obtained, ensuring it is free from organic materials and large particles.
- Approximately 150 grams of soil that has been air-dried and passed through a 425-micron sieve is obtained.
- Distilled water is added to the soil in a mixing dish to create a consistent paste.
- The wet soil paste is then transferred to the cylindrical cup of the cone penetrometer apparatus, ensuring that no air is trapped during the process.
- The soil is leveled up to the top of the cup and positioned on the base of the cone penetrometer apparatus.
- The cone point is adjusted to just touch the surface of the soil paste in the cup, and the initial reading is recorded.
- The vertical clamp is released, allowing the cone to penetrate the soil paste for 5 seconds under its own weight.
- After 5 seconds, the penetration depth of the cone is recorded to the nearest millimeter.

- The test is repeated at least four times, with the penetration values ranging from 14 to 28 mm.
- The exact moisture content of each trial is determined.
- Using the obtained values, a graph is constructed with water content plotted on a regular scale and penetration plotted on a logarithmic scale. A line that best fits the experimental points is drawn on the graph. From this graph, the water content value corresponding to a 20 mm cone penetration is determined, and that value is considered as the liquid limit of the soil.

Plastic limit:

- The air-dried soil sample is placed on the glass plate and any large aggregates broken up
- Water added gradually and the soil mixed thoroughly with a spatula until it reaches a uniform consistency.
- A small portion of the mixed soil sample taken and it is rolled between the palms of your hands to form a thread approximately 3 mm in diameter.
- Rolling continues until the thread crumbles or breaks. This process is repeated with additional soil samples until consistent results are obtained.
- A portion of the crumbled soil is taken and placed in a moisture can for moisture content determination.
- The test is repeated at least three times, so that exact moisture content of each trial is determined. The average value is the plastic limit.

Data and Calculation:

Moisture content: The moisture content can be calculated as:

$$Moisture\ content\ =\ (Mass\ of\ water\ /\ Mass\ of\ dry\ soil)\ x\ 100\%$$

Liquid limit: The liquid limit is the moisture content value corresponding to a 20 mm cone penetration.

Plastic limit: The plastic limit is the average of the moisture content values.

Plasticity Index: The Plasticity index can be calculated as:

$$Plasticity\ Index\ =\ Liquid\ Limit\ -\ Plastic\ Limit$$

Liquidity Index: The Liquidity Index can be calculated as:

$$Liquidity\ Index\ =\ (Natural\ Moisture\ Content\ -\ Plastic\ Limit)\ /\ (Liquid\ Limit\ -\ Plastic\ Limit).$$

Consistency Index: The Consistency Index can be calculated as:

$$Consistency\ Index = (Liquid\ Limit - Natural\ Moisture\ Content) / (Liquid\ Limit - Plastic\ Limit)$$

Soil Consistency: The soil consistency can be obtained from the table below:

Table 1: Soil Consistency

Consistency Stage	Description	Ic	IL	UCS (KN/m^2)
Liquid	Liquid	<0	>1	-------
Plastic	Very soft	0 – 0,25		0-25
	Soft	0,25 – 0, 5		25-50
	Medium Stiff	0,5 – 0,75		50-100
	Stiff	0, 75 - 1		100-200
Semi solids	Very stiff to hard	>1	<0	200-400
Solid	Hard to very hard	>1	<0	>400

Source: Author's own based on literature review

Soil classification: Soil classification (According ISO 14688-2) can be obtained from the chart given in Figure 3.

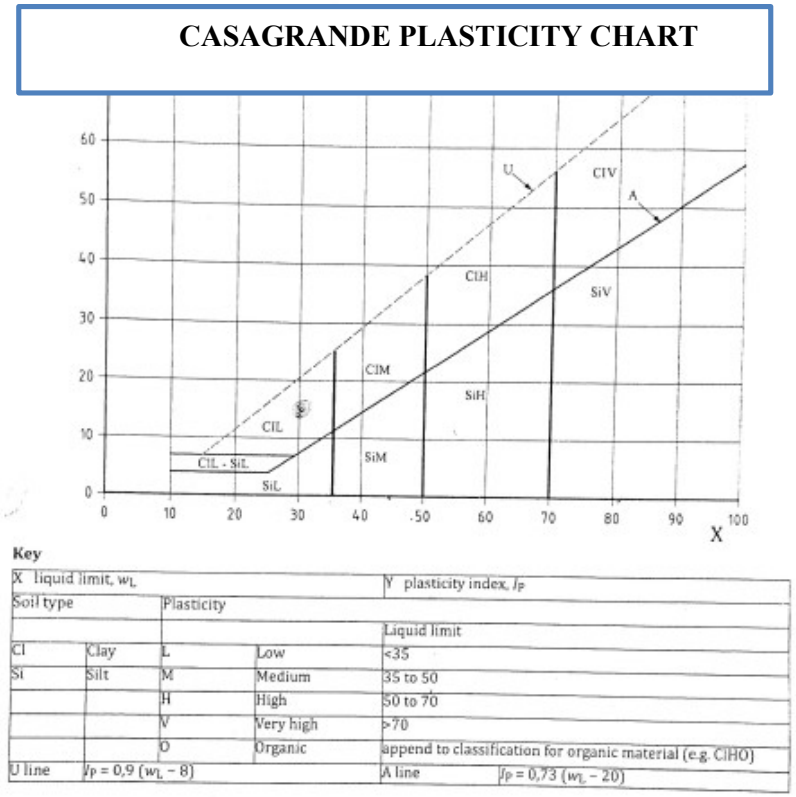

Key

X liquid limit, w_L				Y plasticity index, I_P
Soil type		Plasticity		
				Liquid limit
Cl	Clay	L	Low	<35
Si	Silt	M	Medium	35 to 50
		H	High	50 to 70
		V	Very high	>70
		O	Organic	append to classification for organic material (e.g. ClHO)
U line	$I_P = 0{,}9\ (w_L - 8)$		A line	$I_P = 0{,}73\ (w_L - 20)$

Figure 3: Soil classification (According ISO 14688-2)

Source: Lekstutytė et al, 2023

The soil samples for testing and analysis were taken as four samples from Kelmė 19-1 (depth 9.5-10.0 m), four samples from Kelmė 19-2 (depth 16.6-17.0 m) and 4 samples from Kelmė 37-2 (depth 6.5-7.0 m).

The boreholes data of Kelmė 19 – 1, Kelmė 19 – 2 and Kelmė 37 – 2 was analysed for the determination of consistency limits and the results were obtained (Appendix 1). The results conclude that the investigated soil at 9.5 - 10.0 depth is sandy low plasticity clay. The results conclude that the investigated soil at 16.6 - 17.0 depth is medium plasticity clay. The results conclude that the investigated soil at 6.5 - 7.0 depth is medium plasticity clay.

2.3. Bulk Density 17892-2:2014 & Water Content ISO 17892-1:2014

The determination of bulk density and water content are essential tests conducted on soil samples in geotechnical engineering. These tests provide crucial information about the physical properties and behavior of soils. The bulk density test determines the mass per unit volume of a soil sample, while the water content test determines the amount of water present in the soil. These tests are conducted according to the ISO 17892-2:2014 and ISO 17892-1:2014 standards, respectively (Gribulis et al, 2019).

The purpose of the bulk density test is to determine the mass per unit volume of a soil sample. This information helps in assessing soil compaction, porosity, and stability, and is essential for various engineering applications, such as designing foundations, calculating earth pressures, and evaluating slope stability. The water content test aims to determine the moisture content of a soil sample, which is vital for understanding its behavior, predicting its compaction characteristics, and assessing its suitability for construction purposes (Håkansson & Lipiec, 2000).

Apparatus:

- Balance: A balance with sufficient accuracy to measure the mass of the soil sample.
- Container: A cylindrical container of known volume to hold the soil sample.
- Tamper: A tamper or compacting rod to ensure uniform compaction of the soil sample.
- Oven: An oven to dry the soil sample at a specified temperature.
- Moisture cans: Small, airtight containers to hold soil samples for moisture content determination.

Procedure:

Bulk Density:

- Clean and dry the container. Measure and record its volume.
- Place the container on the balance and record its mass.

- Fill the container with a representative soil sample, ensuring it is compacted uniformly.
- Place the container with the soil on the balance and record its mass.
- Subtract the mass of the empty container from the mass of the container with soil to obtain the mass of the soil. Divide the mass of the soil by the volume of the container to calculate the bulk density.

Water Content:

- Place a clean and dry container on the balance and record its mass.
- Take a sufficient amount of soil sample and record its mass.
- Place the soil sample in the container and record the combined mass of the container and soil.
- Place the container with the soil sample in an oven at a specified temperature until it reaches a constant mass.
- Remove the container from the oven and allow it to cool. Weigh the container with the dried soil sample and record its mass.
- Subtract the mass of the dried soil sample from the combined mass of the container and soil sample. Divide the difference by the mass of the dried soil sample and multiply by 100% to calculate the water content.

Data and Calculations:

Bulk Density:

The bulk density can be calculated as;

$$Bulk\ Density\ =\ Bulk\ Mass\ of\ Soil\ /\ Volume$$

Water Content:

The water content can be calculated as;

$$Moisture\ content\ =\ (Mass\ of\ water\ /\ Mass\ of\ dry\ soil)\ x\ 100\%$$

The results of the tests at different depths of borehole are provided in Appendix 2.

2.4. Incremental Loading Oedometer Test ISO 17892-5:2004

The purpose of the incremental loading oedometer test conducted according to ISO 17892-5:2004 is to determine the consolidation characteristics of a soil sample. This information is vital for assessing the settlement behavior and time-dependent deformation of soils, which is crucial in the design of foundations, embankments, and other geotechnical structures. By understanding the soil's consolidation properties, engineers can make informed decisions regarding construction techniques, settlement predictions, and the overall stability of the soil (Okewale & Grobler, 2023).

Apparatus:

- Oedometer cell, a specialized cell consisting of a rigid ring and a porous stone plate to hold the soil sample.
- Load frame, a mechanical or hydraulic system to apply vertical loads to the soil sample.
- Dial gauges, Precision instruments used to measure the settlement of the soil sample.
- Water reservoir, a container to supply water to the soil sample for saturation.
- Consolidation ring, a ring to confine the soil sample during the test.
- Balance, a balance with sufficient accuracy to measure the mass of the soil sample and other components.

Procedure:

- Prepare a representative soil sample by obtaining an undisturbed or remolded sample from the field. Ensure the sample is free from large particles and organic material.
- Place the soil sample in the oedometer cell and saturate it by allowing water to flow through the porous stone plate. Ensure complete saturation of the sample by maintaining a constant water level above the sample.
- Place the saturated soil sample in the consolidation ring within the oedometer cell. Apply a small initial load and ensure the sample is evenly distributed within the ring.
- Apply successive increments of vertical load to the soil sample at specified time intervals. Allow sufficient time for each increment to allow for settlement and consolidation.
- Measure the settlement of the soil sample at regular intervals using dial gauges or other suitable instruments. Record the settlement values for each applied load increment.
- Plot the settlement versus the square root of time curve (Terzaghi's time factor) and determine the slope of the linear portion using suitable methods. Data and Calculations:

Stress:

The stress can be calculated as;

$$Stress, \sigma = \frac{Load}{Area} \qquad (12)$$

Initial Void Ratio:

The initial void ratio can be calculated as:

$$e_0 = (\rho_s/\rho_d) - 1 \qquad (13)$$

Height of Solids:

The height of solids can be calculated as:

$$H_s = \frac{H_0}{(1 + e_0)} \qquad (14)$$

Void Ratio:

The void ratio can be calculated as:

$$e = \frac{(H_f - H_s)}{H_s} \qquad (15)$$

Degree of Saturation:

The degree of saturation can be calculated as:

$$S_r = \frac{W_0 \rho_0}{e_0 \rho_w} \qquad (16)$$

Strain:

The strain can be calculated as:

$$\varepsilon = \frac{(H_0 - H_s)}{H_0} \qquad (17)$$

Oedometer Modulus:

The oedometer modulus can be calculated as:

$$E_{oed} = \frac{\delta \sigma_y}{\delta \varepsilon} \qquad (18)$$

Coefficient of Volume Compressibility:

The coefficient of volume compressibility can be calculated as:

$$m_v = \left[(H_i - H_f)/H_i\right] * \left(\frac{1000}{\delta \sigma_v}\right) \qquad (19)$$

Compression Index:

The compression index can be calculated as:

$$C_c = \frac{\delta ln \sigma_v}{\delta \varepsilon} \qquad (20)$$

Coefficient of Consolidation:

The coefficient of consolidation can be calculated as:

$$c_v = \frac{0.848 L^2}{t_{90}} \qquad (21)$$

ISO 17892-5:2004 defines the procedures for conducting the incremental loading oedometer test and provides specific guidelines for evaluating the consolidation behaviour of soils under incremental vertical loads. This test is essential for geotechnical engineers to make informed decisions and predictions regarding soil settlement characteristics. The results of incremental

loading oedometer test for all three samples at different moisture contents and bulk density are provided in Appendix 3.

2.5. Cone Penetration test

The cone penetration test (CPT) was performed according to ISO 22476-1:2022. This test is widely used in geotechnical engineering as an in-situ test to map soil profiles and to assess soil properties. The results of CPT for all three boreholes at specified depths are given in Tables 3-5.

Table 3: CPT Results for GR19-1

Depth (m)	Cone Resistance (qc) MPa	Sleeve Friction (fs) MPa	Friction Ratio, Rf (%)
9.50	1.73	0.022	1.272
9.60	2.07	0.022	1.063
9.70	1.75	0.021	1.200
9.80	1.56	0.015	0.962
9.90	1.52	0.01	0.658
10.00	1.74	0.013	0.747

Table 4: CPT Results for GR19-2

Depth (m)	Cone Resistance (qc) MPa	Sleeve Friction (fs) MPa	Friction Ratio, Rf (%)
16.60	4.360	0.092	2.1
16.70	4.070	0.097	2.4
16.80	4.270	0.111	2.6
16.90	4.530	0.105	2.3
17.00	4.900	0.106	2.2

Table 5: CPT Results for GR37-2

Depth (m)	Cone Resistance (qc) MPa	Sleeve Friction (fs) MPa	Friction Ratio, Rf (%)
6.50	1.93	0.18	9.48
6.60	1.69	0.05	2.66
6.70	1.42	0.04	3.03
6.80	1.27	0.04	2.83
6.90	1.14	0.03	2.72
7.00	1.57	0.03	2.04

2.6. Linear regression analysis, multinomial logistic regression model analyses and correlation

Regression analysis is a statistical method used to determine the relationship between variables that have a cause-and-effect connection. In univariate regression, the primary objective

is to examine the association between a single dependent variable and one independent variable, ultimately establishing a linear equation expressing this relationship. The linear regression model is characterized by its simplicity and interpretability, making it a widely used technique in various fields such as geology, economics, finance, etc. (Uyanık & Güler, 2013).

A multinomial logistic regression model is a statistical technique used to predict the probability of categorical outcomes with more than two levels. Unlike binary logistic regression, which predicts outcomes with only two categories, multinomial logistic regression can handle multiple outcome categories. In this model, the dependent variable is categorical with three or more levels, and the independent variables can be continuous or categorical. The model estimates the probability of each category of the dependent variable relative to a reference category, using a set of predictor variables. The output of a multinomial logistic regression model includes the estimated coefficients for each predictor variable, which indicate the direction and magnitude of their effects on the likelihood of each outcome category. Additionally, the model provides odds ratios or relative risk ratios, which represent the change in odds or risk of each outcome category associated with a one-unit change in the predictor variable. Multinomial logistic regression is commonly used in various fields, including social sciences, epidemiology, marketing, and political science, where the outcome of interest has more than two possible categories (Kwak & Clayton-Matthews, 2002).

To perform calculations for determining the relationship of oedometer modulus on cone tip resistance (q_c), the steps provided in Figure 4 should be followed.

Figure 4: Steps of calculation for determining relationship of oedometer modulus on CPT

To create a regression model of the oedometric modulus (E_{oed}) of soil mixtures without regressors of fine fraction (clay) and natural water content (w) under 0.625 MPa stress for samples Kelmė 19-1 and Kelmė 19-2, the following steps have been followed:

- Data for E_{oed}, clay content, water content, and other relevant variables for samples Kelmė 19-1 and Kelmė 19-2 under 0.625 MPa stress collected.
- The data is organized into a format suitable for regression analysis. It has been ensured that measurements for E_{oed}, clay content, and water content for each sample exist.
- Then the coefficient of determination has been used, commonly known as R^2, assesses how well a regression model fits the observed data.
- The regression model is specified, since we are to predict E_{oed} without using clay content and water content (w) as regressors, the model will be of the form:

$$E_{oed} = \beta_0 + \epsilon \qquad (22)$$

  where β_0 is the intercept term and ϵ is the error term.
- Finally, the parameters of the regression model estimated using EViews statistical software and results interpreted.

Cone resistance is a measure of the soil's resistance to penetration by the CPT cone. Higher cone resistance values typically indicate denser and more compacted soils, which tend to have higher oedometer modulus values. The friction ratio is the ratio of the sleeve friction to the cone resistance. It provides information about the soil's shear strength characteristics. Higher friction ratio values may indicate cohesive soils with higher plasticity, which could correlate with lower oedometer modulus values. Pore pressure measurements from the CPT can provide insights into the soil's hydraulic conductivity and drainage characteristics. Elevated pore pressure values may indicate soil layers with lower drainage capability, potentially correlating with lower oedometer modulus values. The classification of soil types encountered during the CPT can also be correlated with oedometer modulus. For example, cohesive soils such as clays may exhibit lower oedometer modulus values compared to granular soils such as sands. The depth at which the CPT measurements are taken can also influence the correlation with oedometer modulus. Deeper soil layers may have undergone greater consolidation and may exhibit higher oedometer modulus values (Sharma et al, 2017).

CHAPTER 3

ANALYSIS OF THE ENGINEERING GEOLOGICAL CROSS-SECTIONS OF KELMĖ REGION

3.1. Kelmė 19 – 1

There are very few research works carried out on engineering geological cross-sections of Kelmė 19-1. According to Geotestus report at depth 1 - 4,9 the soil type is clay of medium plasticity, the colour is gray-brown and it has medium strength. At depth from 2.0 m, the soil shows itself with layers of watery sand. At depth from 4.3 m, the soil type is with abundant dust. At depth 4,9 – 5,7 it is medium sized gravel, brownish yellow, very dense, watery, with boulders. In the interval 5.8-6.0, it is silty clay of low plasticity (morainic), gray, of medium strength, with rather dense, with layers of sand of various shapes. At the depth from 18.7 m, it is dense, with layers of clay and at depth 22 m, it is low-plasticity clay and dust, brown, strong, saturated with water, with watery dusty sand and dusty clay. At depth from 24.6 m, it is dusty sand, yellowish, dense, watery. For detailed information about the layers and cross-sections, it can be referred to Appendix 4.

3.2. Kelmė 19 – 2

From surface to 1.5 m, it is clay of medium plasticity, gray-brown, medium strength, from 1.7 m, it is watery with sand layers. At depth from 4.4 m, it comes out with abundant dust. Between 4,9 – 5,7 m depth, it is medium sized gravel, brownish-yellow very dense water with boulders; at depth from 7.0 m, it is strong silty clay of low plasticity (moraine), gray, of medium strength, with chert and gravel up to 3-5%, with watery sand layers. In the interval of 8.7-10.8 m, it has medium strength. Starting from 18.9 m, it is thick dusty sand, gray, very dense, with layers of ruddy sand. Between 22-24 m depth, it is clay and dust of low plasticity, brown, strong, saturated with water, with watery dusty sand and dusty clay. Starting from 27.0 m, it becomes strong, silty clay of low plasticity (moraine), gray, of medium strength, with chert and chert up to 3-5%, with layers of watery sand. At depth from 28.5 m, it comes out with abundant sand. For detailed information about the layers and cross-sections or Kelmė 19-2, it can be referred to Appendix 4.

3.2. Kelmė 37 – 2

It is loamy clay of low plasticity (moraine), reddish-brown, weak, with chert and gravel up to 3.5% till 1.5 m. As of 1.5 m, it is brown and it has medium strength. Starting from 4.3 m, it is gray. As of depth from 6.3 m, it comes out with watery sand slopes. As of depth from 13.6 m, it

becomes strong. For detailed information about the layers and cross-sections or Kelmė 37-2, it can be referred to Appendix 4.

Overall, the soil profile exhibits a diverse range of soil types, including clay, gravel, silty clay, sandy soil, and dusty sand, with varying degrees of plasticity, strength, and water content across different depth intervals.

CHAPTER 4

ANALYSIS OF THE RESULTS

4.1. Research process: regression analysis and correlation

The examined glacial till soil has a complex structure, as shown by its varying strength (as measured by q_c and f_s) and physical qualities; this, in turn, accounts for the database's complexity. To enhance the accuracy of the study results and to uncover relationships between Oedometric modulus and cone penetration soil parameters, the soil that was being studied was separated into subgroups and then analyzed. For the purpose of grouping soils, Robertson's (Robertson 2016) soil behavior type (SBT) was selected. This type specifies the boundaries between zones of different soil behavior types under stress and load. This criterion is highly helpful for evaluating soil mechanical qualities since it distinguishes between cohesive (clayey) and non-cohesive (sandy) soils and also helps to define their boundaries. Even if you don't know the precise distribution of soil grains or their plasticity, you may still use it to characterize the type of soil. A case study on liquefaction susceptibility (Green, Ziotopoulou, 2015) proved that this metric is reliable. There were two primary categories of soil behavior in the till soil that was analyzed, based on the soil behavior index I_c: clayey silt to silty clay and clay to silty clay. When the amount of clay in the soil is less than 10-15%, the examination of soil behavior revealed that grain size distribution does not contribute to the differentiation of soil behavior types by I_c. Soil plasticity characteristics, however, have a more significant effect on the I_c index. Soil typically consists of a combination of clay, silt, sand, and gravel. Soil layers are separated based on cone penetration data (q_c and R_f) as shown in figures 11, 12, and 13.

The Robertson soil behavior index (SBT) was computed for the purpose of further study (Robertson 2016). Soil samples were categorized into two groups according to their I_c indicators, which represent different forms of soil behavior:

Very stiff to hard clay (I_c = 1.16 -1.17)

Stiff clay (I_c = 0.98)

Afterwards, each I_c group was subdivided according to the 1-5 MPa cone resistance (q_c), in accordance with P.K. Robertson's soil categorization scheme (Robertson 2009). The estimated Oedometric modulus (E_{Eoed}) was analyzed using a multinomial logistic regression model. This model is used to find correlation between different parameters and is a part of statistical data analysis. We use this model to check the dependence of Oedometric modulus to CPT parameters. We run this model based on Oedometric values and qc value from CPT. The relationship between

the soil's characteristics and the determined oedometer modulus (E_{Doed}), which was measured in a laboratory test, was examined and understood. We measured the values of the cone penetration resistance to estimate the E_{Eoed} values. The oedometer modulus was calculated according to the standards set out by EN ISO 17892-5:2017, using the filtered q_c values as a basis.

In the analysis, E_{Doed} and E_{Eoed} were used. Below their definition is provided:

E_{Doed}: This represents the measured oedometer modulus obtained directly from laboratory oedometer tests. It reflects the soil's stiffness or resistance to deformation under vertical stress conditions.

E_{Eoed}: This denotes the effective oedometer modulus, which is calculated based on soil properties using regression analysis. It provides an estimate of the oedometer modulus derived from soil index properties or other parameters instead of direct laboratory testing.

Underneath, the methodology chosen and reason of choosing this methodology is given:

The first step involved selecting a set of predictor variables that are believed to influence the oedometer modulus. Next, a dataset comprising measured oedometer modulus (E_{Doed}) and corresponding q_c properties was added. Regression analysis was then conducted to establish the relationship between E_{Doed} and the selected q_c variables. Both linear and nonlinear regression techniques may be employed, depending on the nature of the relationship between the variables. In our case linear regression techniques were used.

As part of the investigation, regression equations were developed to determine the optimal soil property-based relationship between the E_{Doed} and the E_{Eoed}. The regression equations developed to establish the relationship between the measured oedometer modulus (E_{Doed}) and the effective oedometer modulus (E_{Eoed}) could be formulated as follows:

Linear Regression Equation:

$$y = mx + b \quad (23)$$

Where,

m – is a slope

b – is an intercept.

Once these regression equations are derived, they are used to predict the relationship between two variables, x and y, in a simple and interpretable manner. The slope m indicates the rate of change in y for a unit change in x, while the intercept c represents the value of y when x is zero.

The oedometer deformation modulus at stress values of 0.039, 0.078, 0.156, 0.312, and 0.625 MPa is shown in the present study. The geotechnical design community heavily relies on these stress magnitudes. It is possible to accurately evaluate the mechanical behavior and

deformation properties of soils at both stress levels. It is consistent with the norm in civil design in Lithuania to use these particular stress levels.

The regression statistics, regression analysis, q_c and intercept calculations, trendline calculations and graphs have been obtained by means of EViews software and other calculation means.

3.2. Cone resistance (q_c), Sleeve friction (f_s) and Rf calculations of Kelmė at different depths

The boreholes data of Kelmė 19 – 1, Kelmė 19 – 2 and Kelmė 37 – 2 was analyzed for the determination of consistency limits and the results were obtained. The results conclude that, at the boreholes, the low plasticity clay (CIL) at depth 9.5 – 10 m and medium plasticity clay (CIM) at depths 16.6 – 17 m & 6.5 – 7 m, respectively were obtained. The soil consistency of stiff was obtained for Kelmė 37-2 sample, very stiff to hard were obtained for Kelmė 19- and Kelmė 19-2 soil samples.

In the Figure 5, distribution of the investigated Pleistocene glacial till soils in P.K. Robertson's (2016) soil behavior type graph with the indicated I_C soil behavior type boundaries is presented.

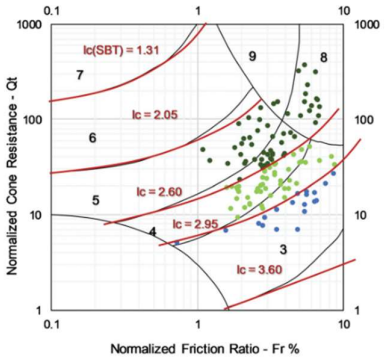

Figure 5: Distribution of the investigated Pleistocene glacial till soils in P.K. Robertson's (2016) soil behaviour type

graph with the indicated I_C soil behaviour type boundaries: 3 – clays, 4 – silt mixture, 5 – sand mixture, 6 – sands, 7 – gravelly sand, 8 – very stiff sand to clayey sand, 9 – very stiff fine-grained sand.

The boreholes data of Kelmė was analyzed for the determination of bulk density & water content and the results were obtained. The bulk density & water content of the CIL and CIM soils for the three different depths on three samples taken from Kelmė 19-1, Kelmė 19-2 and Kelmė 37-2 were calculated.

3.3. Relationship of Oedometric Modulus on Cone Penetration Resistance

The relationship between the oedometer modulus and cone tip resistance (qc) provides insight into the mechanical behavior of soils under load. Typically, as the cone tip resistance (qc) increases, indicating denser and more compacted soils, the oedometer modulus also tends to increase. This correlation suggests that denser soils generally exhibit higher stiffness and resistance to deformation. However, it's important to note that the relationship between oedometer modulus and cone tip resistance (q_c) parameters can vary depending on factors such as soil type, composition, and moisture content. In some cases, other soil properties such as cohesion, friction angle, and compressibility may also influence this relationship.

The Linear Regression by the software was performed using the following formulas:

Slope m: $$m = \left(n * \sum x_i\, y_i - (\sum x_i) * (\sum y_i)\right) / \left(n * \sum x_i^2 - (\sum x_i)^2\right) \quad (24)$$

Intercept b: $$b = \left(\sum y_i - m * (\sum x_i)\right)/n \quad (25)$$

Mean x: $$\bar{x} = \sum x_i / n \quad (26)$$

Mean y: $$\bar{y} = \sum y_i / n \quad (27)$$

Sample correlation coefficient r:

$$r = \left(n * \sum x_i y_i - (\sum x_i)(\sum y_i)\right) / \sqrt{[n * \sum x_i^2 - (\sum x_i)^2][n * \sum y_i^2 - (\sum y_i)^2]} \quad (28)$$

$$-1 < r < +1$$

Where:

n is the total number of samples,

x_i $(x_1, x_2, \ldots, x_n)$ are the x values,

y_i $(y_1, y_2, \ldots, y_n)$ are the y values,

$\sum x_i$ is the sum of x values,

$\sum y_i$ is the sum of y values,

$\sum x_i y_i$ is the sum of products of x and y values,

$\sum x_i^2$ is the sum of squares of x values,

$\sum y_i^2$ is the sum of squares of y values.

Table 6 gives calculations of q_c and E_{oed} values of Kelmė 19-1 at different stress levels.

Table 6: q_c and E_{oed} values of Kelmė 19-1 for Scatter plot trendline

q_c, x-axis	**E_{oed}, y-axis**	Stress (kPa)
1.73	2.516	39
2.07	1.663	78
1.75	2.332	156
1.56	3.377	312
1.74	5.269	625

Figure 9 illustrates scatter plot and line of best fit of q_c and E_{oed} for Kelmė 19-1 calculated by means of Geography Field Work Calculator.

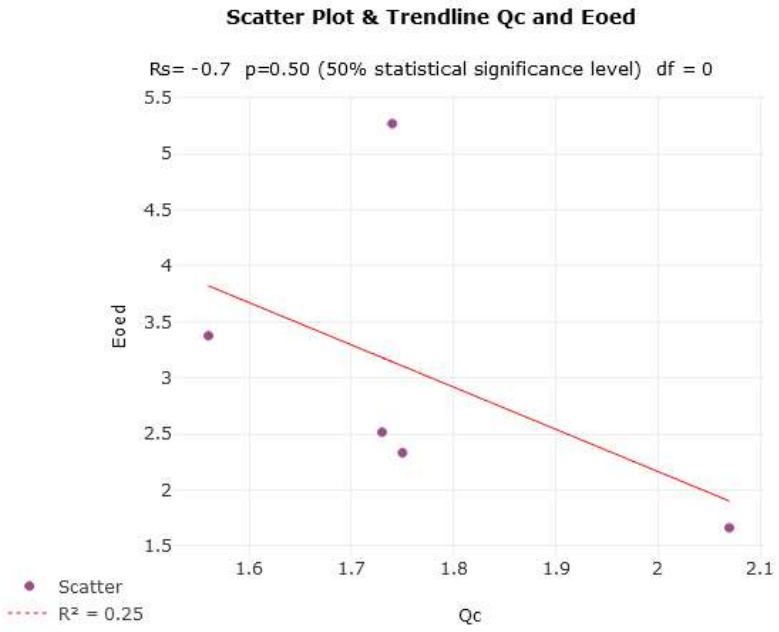

Figure 6: Scatter Plot trendline for Kelmė 19-1 q_c & E_{oed} relation based on Geography Field Work Calculator

Rs value: -0.7

Critical p (probability) value and significance level: p=0.50 (50% statistical significance level)

Degrees of freedom: degrees of freedom = 0

There appears to be a strong negative correlation Rs value (-0.7). There is a 50% probability that null hypothesis is correct p=0.50 (50% statistical significance level). So the null hypothesis must be accepted that there is no correlation.

Figure 7 illustrates scatter plot and line of best fit of q_c and E_{oed} for Kelmė 19-1 calculated by means of Stats Suite Simple Linear Regression Calculator.

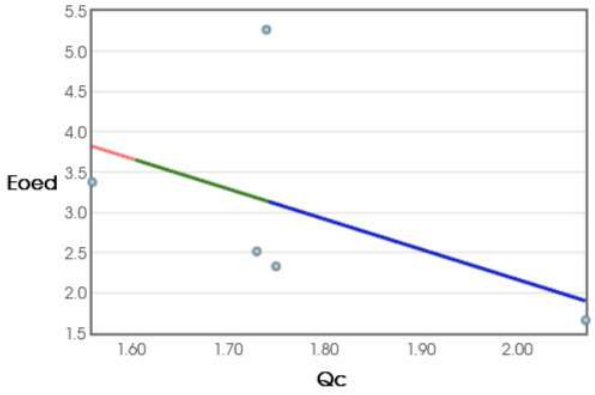

Figure 7: Scatter Plot trendline for Kelmė 19-1 q_c & E_{oed} relation based on Stats Suite Simple Linear Regression Calculator

Regression Line: $Eoed = -3.763649635 \cdot qc + 9.693059854$

Correlation: $r = -0.5002850408$

R-squared: $r^2 = 0.250285122$

The correlation coefficient (r) is -0.5002850408, indicating a moderate negative correlation between qc and Eoed. This suggests that as qc increases, Eoed tends to decrease moderately, and vice versa. The coefficient of determination (R^2) is 0.250285122, which represents the proportion of the variance in Eoed that is explained by the linear regression model. In this case, approximately 25.03% of the variability in Eoed can be explained by the variability in qc.

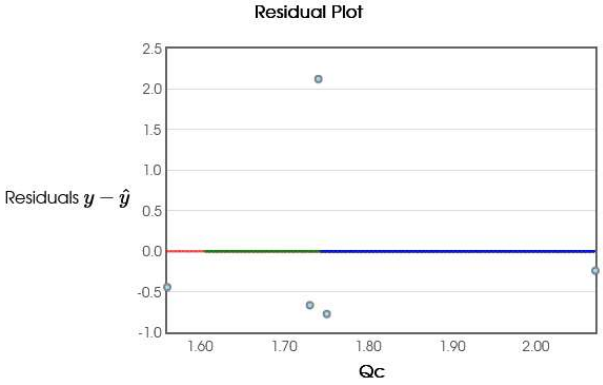

Figure 8: Residual plot for Kelmė 19-1 based on Stats Suite Simple Linear Regression Calculator

Figure 8 illustrates residual plot for Kelmė 19-1.

Regression Inference: $y = \alpha + \beta x$

Degrees of Freedom: $df = n - 2 = 3$

Estimate of Slope: $b = -3.763649635$

Standard Error Slope: $SEb = 3.7607902102$

Regression Standard Error: $s = 1.3920004999$

t-Statistic: $t = -1.0007603255$

95% Confidence Interval for β: $(-3.763649635, -3.763649635)$

p-value: $p = 0.390688$

Assuming that the true slope is $\beta = 0$, the probability of seeing a test statistic as far out as $t = -1.0007603255$ is 0.390688.

That is, assuming that there is no straight-line relationship between q_c and E_{oed}, 39.1% of all similarly collected samples would have a test statistic as far away from 0 as $t = -1.0007603255$.

Conclusion: Keep the null hypothesis. $(0.390688 = p \geq \alpha = 0.05)$

Figure 9 illustrates polynomial plot q_c and E_{oed} for Kelmė 19-1 calculated by means of Stats Suite Polynomial Regression Calculator.

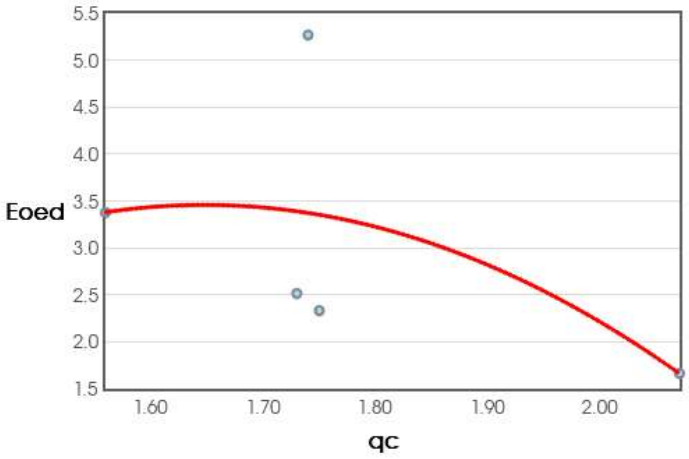

Figure 9: Scatter plot trendline for Kelmė 19-1 based on Stats Suite Stats Suite Polynomial Regression Calculator

Regression Polynomial: $E_{oed} = -10.0951 \cdot qc^2 + 33.2728 \cdot q_c - 23.9579$

R-squared: $r^2 = 0.3032$

Adjusted R-squared: $r^2_{adj} = 0.0709$

Residual Standard Error: 1.6436 on 2 degrees of freedom

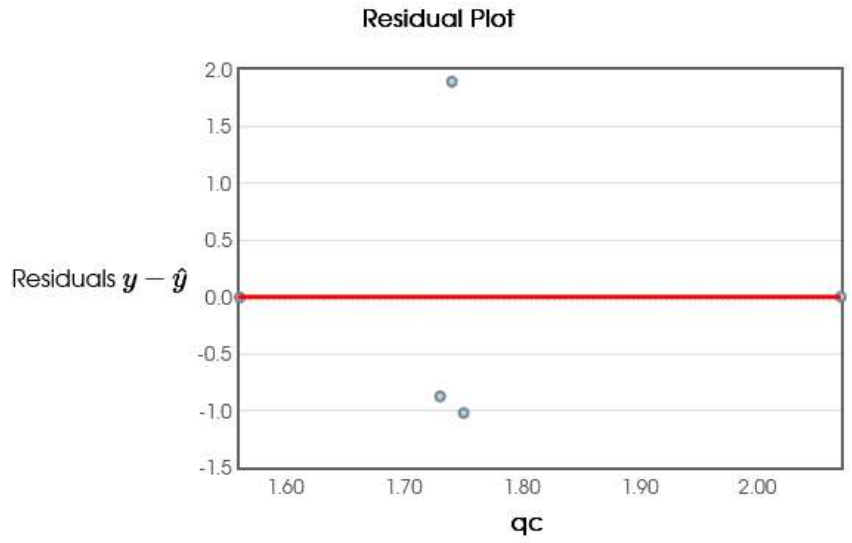

Figure 10: Residual plot for Kelmė 19-1 based on Stats Suite Stats Suite Polynomial Regression Calculator

Figure 10 provides residual plot for Kelmė 19-1 and Table 7 provides polynomial linear regression calculation results for Kelmė 19-1.

Table 7: Analysis of Variance Table

Coefficient	Estimate	Standard Error	t-statistic	p-value
β_0	-23.9579	86.7378	-0.2762	0.8083
β_1	33.2728	86.7378	-0.2762	0.76
β_2	-10.0951	25.9128	-0.3896	0.7344

Source	df	SS	MS	F-statistic	p-value
Regression	2	2.3506	1.1753	0.4351	0.6968
Residual Error	2	5.403	2.7015		
Total	4	7.7536	1.9384		

This polynomial equation suggests a quadratic relationship between E_{oed} and q_c, indicating that the relationship is not purely linear but involves a squared term of q_c. $R^2 = 0.3032$ indicates that approximately 30.32% of the variance in E_{oed} can be explained by the quadratic regression model. The adjusted R^2 value ($R_{adj}^2 = 0.0709$) adjusts for the number of predictors in the model, providing a more conservative estimate of the model's explanatory power. The residual standard error (RSE=1.6436) is an estimate of the standard deviation of the residuals (the differences between observed and predicted values). A lower RSE indicates better model fit. The regression

F-statistic tests the null hypothesis that all regression coefficients are equal to zero. In this case, the F-statistic value (0.4351) with its associated p-value (0.6968) suggests that the regression model as a whole is not statistically significant at the conventional significance level of 0.05. The p-values for individual coefficients (β0, β1, β2) indicate whether each coefficient is statistically significant. In this case, none of the coefficients are statistically significant, as their p-values are all greater than 0.05.

Table 8 shows calculations of q_c and E_{oed} values of Kelmė 19-2 at different stress levels.

Table 8: q_c and E_{oed} values of Kelmė 19-2 for Scatter plot trendline

q_c, x-axis	**E_{oed}, y-axis**	Stress (kPa)
2.1	3.25	39
1.81	1.912	78
1.91	2.342	156
1.7	2.897	312
1.83	4.148	625

Figure 11 illustrates scatter plot and line of best fit of q_c and E_{oed} for Kelmė 19-2.

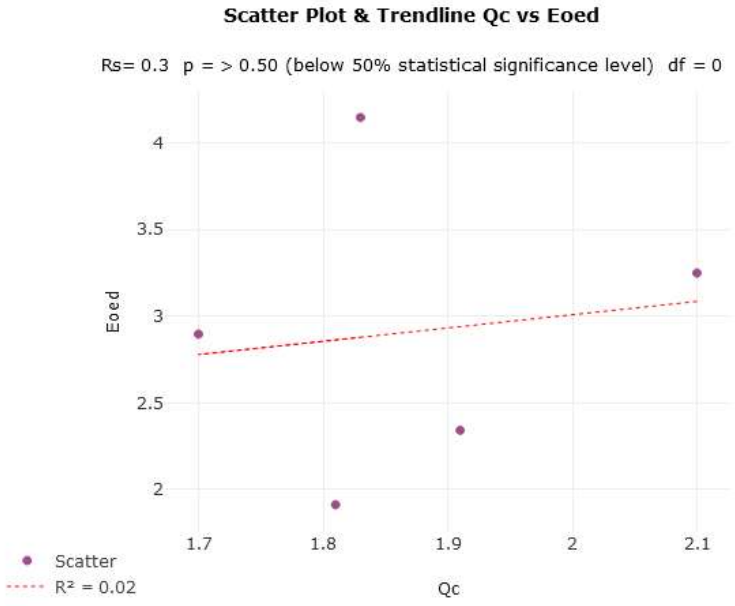

Figure 11: Scatter Plot trendline for Kelmė 19-2 q_c & E_{oed} relation based on Geography Field Work Calculator

Rs value: 0.3

Critical p (probability) value and significance level: p = > 0.50 (below 50% statistical significance level)

Degrees of freedom: degrees of freedom = 0

There appears to be a weak positive correlation Rs value (+0.3). There is a greater than 50% probability that the null hypothesis is correct p = > 0.50 (below 50% statistical significance level). So, the null hypothesis must be accepted that there is no correlation.

Figure 12 illustrates scatter plot and line of best fit of q_c and E_{oed} for Kelmė 19-2 calculated by means of Stats Suite Simple Linear Regression Calculator.

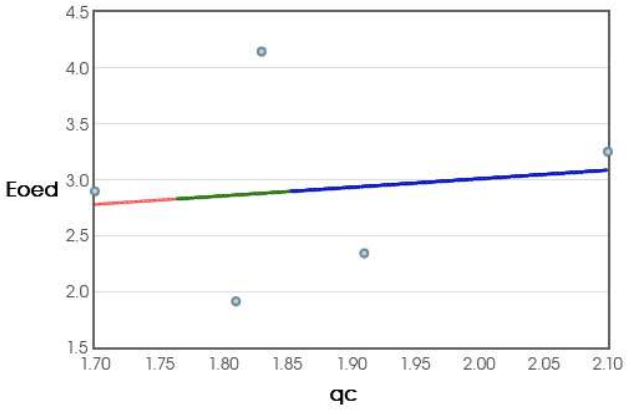

Figure 12: Scatter Plot trendline for Kelmė 19-2 q_c & E_{oed} relation based on Stats Suite Simple Linear Regression Calculator

Regression Line: $E_{oed} = 0.7681 \cdot qc + 1.4735$

Correlation: r =0.1327

R-squared: r^2=0.0176

for μy at x=: 1.7

for y at x=: 1.7

The correlation coefficient (r) is 0.1327, indicating a weak positive correlation between qc and E_{oed}. This suggests that as qc increases, E_{oed} tends to increase slightly, but the relationship is not very strong. The coefficient of determination (R^2) is 0.0176, which represents the proportion of the variance in E_{oed} that is explained by the linear regression model. In this case, only approximately 1.76% of the variability in E_{oed} can be explained by the variability in q_c.

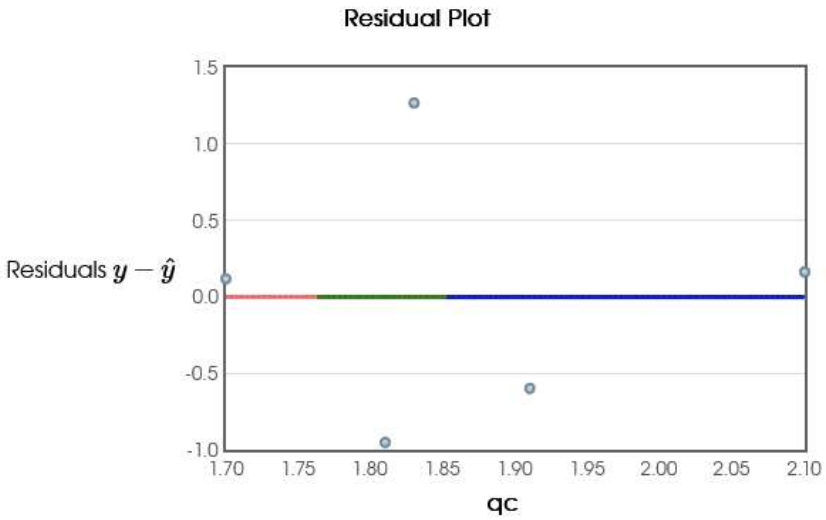

Figure 13: Residual plot for Kelmė 19-2 based on Stats Suite Simple Linear Regression Calculator

Regression Inference: $y = \alpha + \beta x$

Degrees of Freedom: $df = n - 2 = 3$

Estimate of Slope: $b = 0.7681$

Standard Error Slope: $SEb = 3.3115$

Regression Standard Error: $s = 0.9857$

t-Statistic: $t = 0.2319$

95% Confidence Interval for β: $(0.7681, 0.7681)$

p-value: $p = 0.8315$

Assuming that the true slope is β=0, the probability of seeing a test statistic as far out as t=0.2319 is 0.8315. That is, assuming that there is no straight-line relationship between q_c and E_{oed}, 83.2% of all similarly collected samples would have a test statistic as far away from 0 as t=0.2319. Conclusion: Keep the null hypothesis. (0.8315=p≥α=0.05)

Figure 14 illustrates polynomial plot q_c and E_{oed} for Kelmė 19-2 calculated by means of Stats Suite Polynomial Regression Calculator.

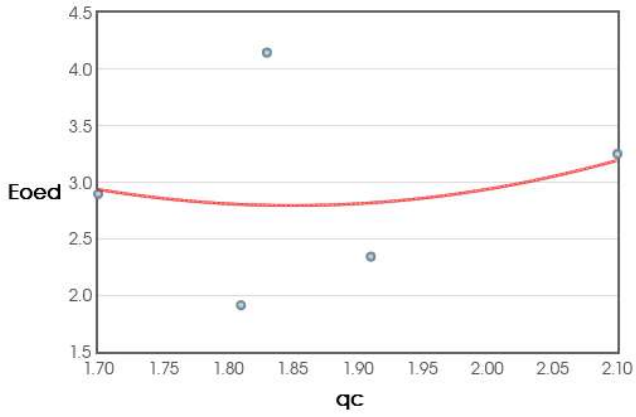

Figure 14: Scatter plot trendline for Kelmė 19-2 based on Stats Suite Stats Suite Polynomial Regression Calculator

Regression Polynomial: $E_{oed} = 6.3716 \cdot qc^2 - 23.5678 \cdot qc + 24.5879$

R-squared: $r^2 = 0.0384$

Adjusted R-squared: $r^2_{adj} = -0.2821$

Residual Standard Error: 1.1944 on 2 degrees of freedom

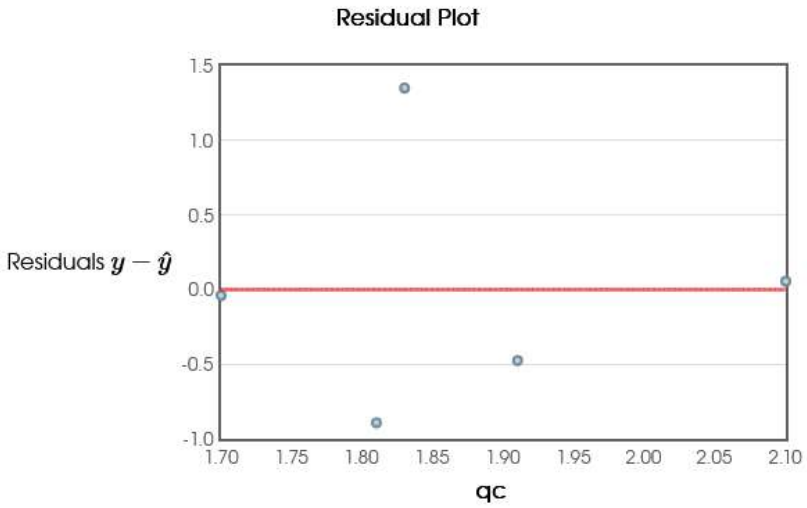

Figure 15: Residual plot for Kelmė 19-2 based on Stats Suite Stats Suite Polynomial Regression Calculator

Figure 15 provides residual plot for Kelmė 19-2 and Table 9 provides polynomial linear regression calculation results for Kelmė 19-2.

Table 9: Analysis of Variance Table

Coefficient	Estimate	Standard Error	t-statistic	p-value
β_0	24.5879	111.2917	0.2209	0.8457

β_1	-23.5678	116.9739	-0.2015	0.859
β_2	6.3716	30.6079	0.2082	0.8544

Source	**df**	**SS**	**MS**	**F-statistic**	**p-value**
Regression	2	0.1141	0.057	0.04	0.9616
Residual Error	2	2.853	1.4265		
Total	4	2.967	0.7418		

The provided regression analysis includes polynomial regression models for estimating the relationship between q_c (cone penetration resistance) and E_{oed} (deformation modulus) for Kelmė 19-2, along with residual plots and ANOVA tables. R^2=0.0384 indicates that only approximately 3.84% of the variance in E_{oed} is explained by the polynomial regression model. The adjusted R^2 value (R_{adj}^2=−0.2821) is negative, suggesting that the model's explanatory power is poor and potentially overfitting the data. The residual standard error (RSE=1.1944) is an estimate of the standard deviation of the residuals (the differences between observed and predicted values). It's relatively small compared to the observed values, but the poor R^2 suggests that the model might not be capturing the true relationship. The ANOVA table provides information about the significance of the regression model. The regression F-statistic tests the null hypothesis that all regression coefficients are equal to zero. In this case, the F-statistic value (0.04) with its associated p-value (0.9616) suggests that the regression model as a whole is not statistically significant at the conventional significance level of 0.05. The p-values for individual coefficients (β0, β1, β2) indicate whether each coefficient is statistically significant. In this case, none of the coefficients are statistically significant, as their p-values are all greater than 0.05.

Table 10 provides calculations of q_c and E_{oed} values of Kelmė 37-2 at different stress levels.

Table 10: q_c and E_{oed} values of Kelmė 37-2 for Scatter plot trendline

q_c, x-axis	**E_{oed}, y-axis**	Stress (kPa)
1.69	3.697	39
1.42	2.422	78
1.27	3.197	156
1.14	4.413	312
1.57	6.394	625

Figure 16 illustrates scatter plot and line of best fit of q_c and E_{oed} for Kelmė 37-2.

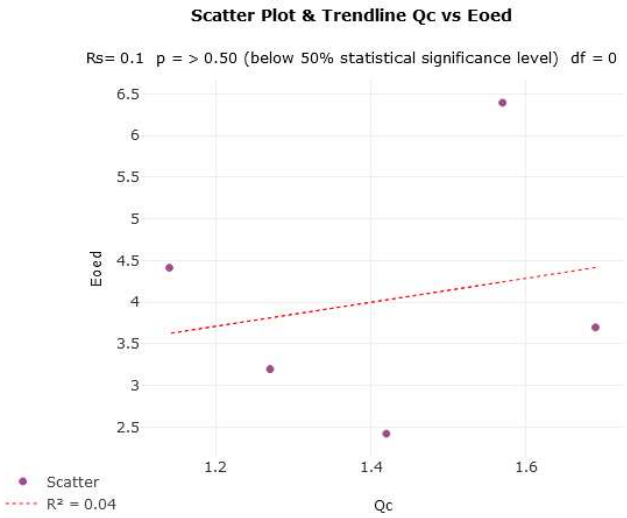

Figure 16: Scatter Plot trendline for Kelmė 37-2 q_c & E_{oed} relation

Rs value: 0.1

Critical p (probability) value and significance level: p = > 0.50 (below 50% statistical significance level)

Degrees of freedom: degrees of freedom = 0 There appears to be a very weak positive correlation Rs value (+0.1).

There is a greater than 50% probability that the null hypothesis is correct p = > 0.50 (below 50% statistical significance level). So, the null hypothesis must be accepted that there is no correlation.

Figure 17 illustrates scatter plot and line of best fit of q_c and E_{oed} for Kelmė 37-2 calculated by means of Stats Suite Simple Linear Regression Calculator.

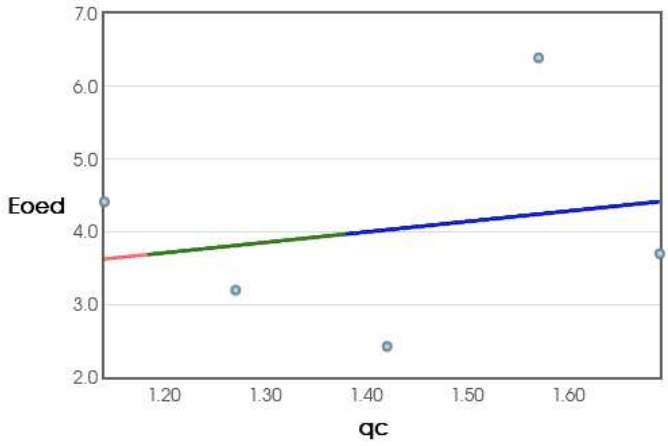

Figure 17: Scatter Plot trendline for Kelmė 37-2 q_c & E_{oed} relation based on Stats Suite Simple Linear Regression Calculator

Regression Line: $E_{oed} = 1.4385 \cdot qc + 1.9848$

Correlation: r =0.211

R-squared: r^2=0.0445

for μy at x=: 1.7

for y at x=: 1.7

The correlation coefficient (r) is 0.211, indicating a weak positive correlation between q_c and E_{oed}. This suggests that as q_c increases, E_{oed} tends to increase slightly, but the relationship is not very strong. The coefficient of determination (R^2) is 0.0445, which represents the proportion of the variance in E_{oed} that is explained by the linear regression model. In this case, only approximately 4.45% of the variability in Eoed can be explained by the variability in qc.

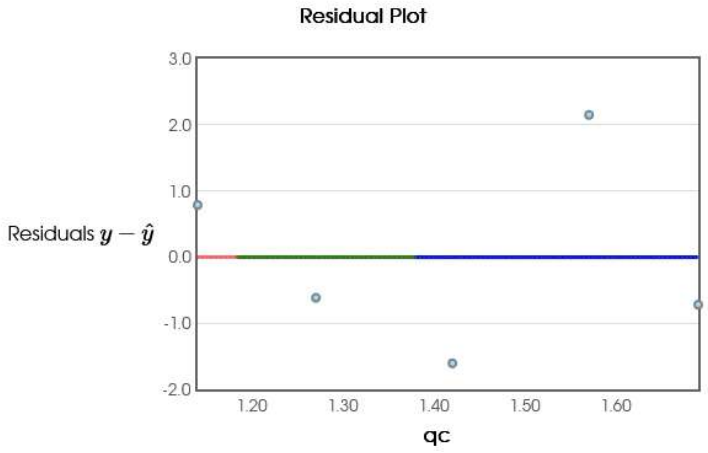

Figure 18: Residual plot for Kelmė 37-2 based on Stats Suite Simple Linear Regression Calculator

Regression Inference: $y = \alpha + \beta x$

Degrees of Freedom: $df = n - 2 = 3$

Estimate of Slope: $b = 0.4385$

Standard Error Slope: $SEb = 3.8481$

Regression Standard Error: $s = 1.7048$

t-Statistic: $t = 0.3738$

95% Confidence Interval for β: $(1.4385, 1.4385)$

p-value: $p = 0.7334$

Assuming that the true slope is β=0, the probability of seeing a test statistic as far out as t=0.3738 is 0.7334. That is, assuming that there is no straight-line relationship between q_c and E_{oed}, 73.3% of all similarly collected samples would have a test statistic as far away from 0 as t=0.3738. Conclusion: Keep the null hypothesis. (0.7334=p≥α=0.05)

Figure 19 illustrates polynomial plot q_c and E_{oed} for Kelmė 37-2 calculated by means of Stats Suite Polynomial Regression Calculator.

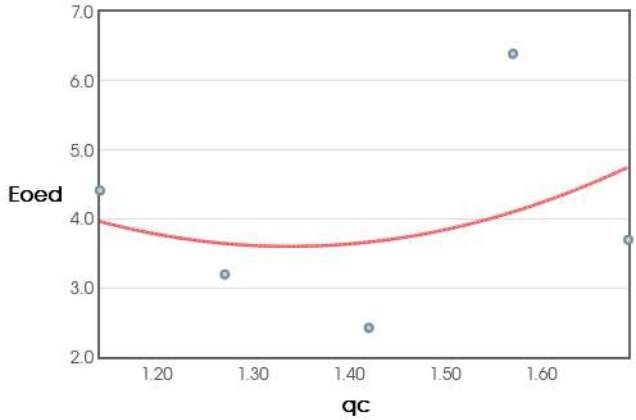

Figure 19: Scatter plot trendline for Kelmė 37-2 based on Stats Suite Stats Suite Polynomial Regression Calculator

Regression Polynomial: $E_{oed} = 9.2567 \cdot qc^2 - 24.7621 \cdot qc + 20.1612$

R-squared: $r^2 = 0.0891$

Adjusted R-squared: $r^2_{adj} = -0.2145$

Residual Standard Error: 2.0387 on 2 degrees of freedom

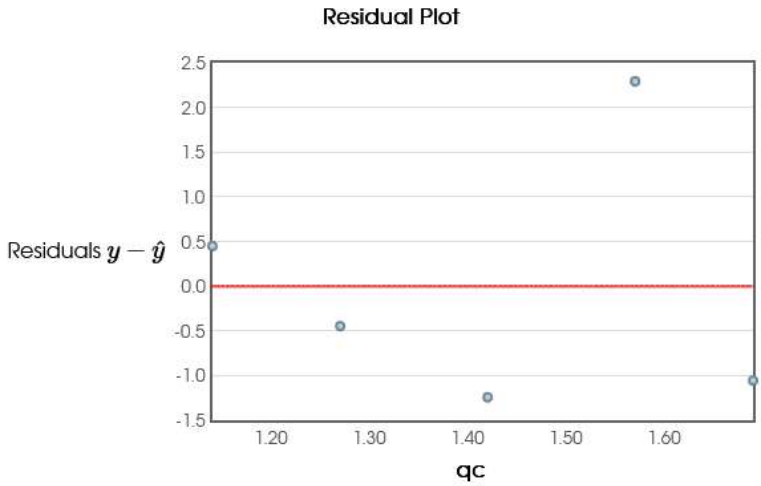

Figure 20: Residual plot for Kelmė 37-2 based on Stats Suite Stats Suite Polynomial Regression Calculator

Figure 20 provides residual plot for Kelmė 37-2 and Table 11 provides polynomial linear regression calculation results for Kelmė 37-2.

Table 11: Analysis of Variance Table

Coefficient	Estimate	Standard Error	t-statistic	p-value
β_0	20.1612	58.4631	0.3449	0.7631

β_1	-24.7621	83.8621	-0.2953	0.7956
β_2	9.2567	29.584	0.3129	0.784

Source	df	SS	MS	F-statistic	p-value
Regression	2	0.8131	0.4065	0.0978	0.9109
Residual Error	2	8.3124	4.1562		
Total	4	9.1255	2.2814		

The provided regression analysis presents a polynomial regression model for estimating the relationship between qc (cone penetration resistance) and Eoed (deformation modulus) for Kelmė 37-2, along with residual plots and ANOVA tables. R^2=0.0891 indicates that approximately 8.91% of the variance in Eoed can be explained by the polynomial regression model. The adjusted R^2 value (R_{adj}^2=−0.2145) is negative, which is unusual and could indicate that the model is overfitting the data or that there are issues with model specification. The residual standard error (RSE=2.0387) is an estimate of the standard deviation of the residuals (the differences between observed and predicted values). It's relatively high, suggesting that the model may not be fitting the data well. The ANOVA table provides information about the significance of the regression model. The regression F-statistic tests the null hypothesis that all regression coefficients are equal to zero. In this case, the F-statistic value (0.0978) with its associated p-value (0.9109) suggests that the regression model as a whole is not statistically significant at the conventional significance level of 0.05. The p-values for individual coefficients (β0, β1, β2) indicate whether each coefficient is statistically significant. In this case, none of the coefficients are statistically significant, as their p-values are all greater than 0.05.

3.4. Multinomial logistic regression model analyses of all the distinguished soil behaviour types under 39 kPa (the lowest) and 625 kPa (the highest) stresses

Multinomial logistic regression model analysis of all the distinguished soil behaviour types under the lowest (39 kPa) and the highest (625 kPa) stresses without regressors of fine fraction (clay) and natural water content (w) conducted using EViews software. Figure 15 illustrates results of calculation by means of EViews software.

Table 12: Calculation of E_{oed} and q_c at different depths under 39 MPa stress

Stress (kPa)	E_{oed} (MPa)	Characteristic q_c value (MPa)	Depth, m
39	3.250	1.78	9.5-10.0

39	2.516	1.78	9.5-10.0
39	6.667	6.345	16.6-17.0
39	1.822	6.345	16.6-17.0
39	4.875	6.345	16.6-17.0
39	9.873	6.345	16.6-17.0
39	5.571	1.69	6.5-7.0
39	3.697	1.69	6.5-7.0
39	2.868	1.69	6.5-7.0
39	1.769	1.69	6.5-7.0

qc	Eoed	Ŷ (Predicted Y)	Residual
1.78	3.250	3.314	-0.06402
1.78	2.516	3.314	-0.798
6.345	6.667	5.8051	0.8619
6.345	1.822	5.8051	-3.9831
6.345	4.875	5.8051	-0.9301
6.345	9.873	5.8051	4.0679
1.69	5.571	3.2649	2.3061
1.69	3.697	3.2649	0.4321
1.69	2.868	3.2649	-0.3969
1.69	1.769	3.2649	-1.4959

Legend: y-Predicted values are E_{oed} Predicted values

Figure 21: Regression calculation of oedometric modulus (E_{oed}) of soil mixtures without regressors of fine fraction (clay) and natural water content (w) under 39 kPa stress for all depths on EViews software

Regression line equation

$$\hat{Y} = 2.3427 + 0.5457X$$

Reporting linear regression in APA style

R2 = .26, F(1,8) = 2.87, p = .128.

β = .55, p = .128, α = 2.34, p = .124.

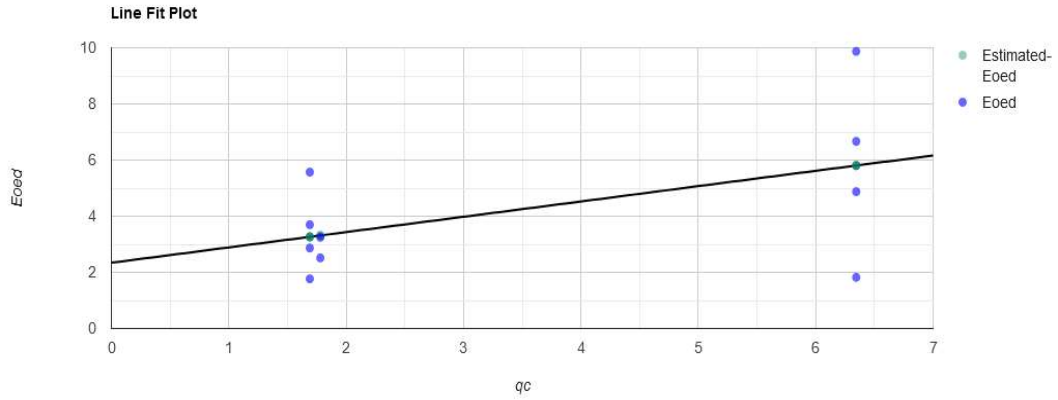

Figure 22: Line Fit Plot of E_{oed} estimated and E_{oed} determined

Figure 22 illustrates line fit plot of E_{oed} estimated and E_{oed} determined. Y-estimated values are E_{oed} estimated, it is given as light blue dots in the figure. Y values are E_{oed} determined values, they are shown as dark blue dots in the figure. Figure 23 provides prediction interval of E_{oed}. Black line shows regression line, blue line is 95% confidence interval and red line is 95% prediction interval.

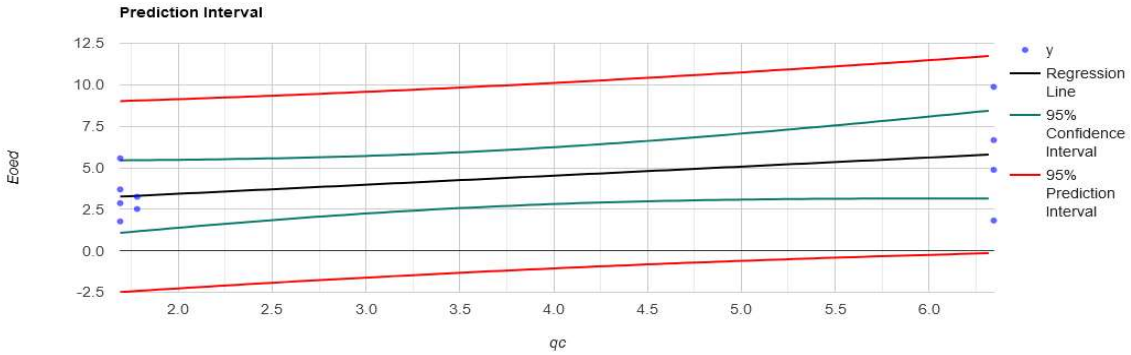

Figure 23: Prediction interval of E_{oed}

Figure 24 illustrated residual plot of E_{oed}.

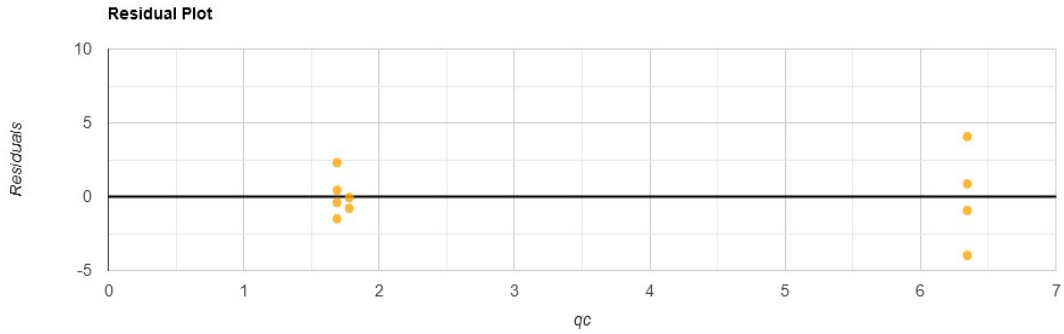

Figure 24: Residual plot of E_{oed}

Source	DF	Sum of Square	Mean Square	F Statistic (df_1,df_2)	P-value
Regression (between $\hat{y}_i$ and $\bar{y}$)	1	15.2902	15.2902	2.874 (1,8)	0.1285
Residual (between y_i and $\hat{y}_i$)	8	42.5618	5.3202		
Total (between y_i and $\bar{y}$)	9	57.8521	6.428		

Figure 25: Regression analysis of E_{oed} in ANOVA

Figure 24 provides ANOVA regression calculation of E_{oed} by means of EViews software.

Explanation of ANOVA regression analysis is as follows:

Eoed and qc relationship under 39 kPa stress

R-Squared (R^2) equals **0.2643.** This means that 26.4% of the variability of E_{oed} is explained by q_c. Correlation (R) equals **0.5141**. This means that there is a **moderate direct relationship** between q_c and E_{oed}. The Standard deviation of the residuals (S_{res}) equals **2.3066**. The slope: b_1=**0.5457** CI[-0.1966, 1.288] means that when you increase q_c by 1, the value of E_{oed} increases by 0.5457. The y-intercept: b_0=**2.3427** CI[-0.796, 5.4813] means that when q_c equals 0, the prediction of E_{oed}'s value is 2.3427. The x-intercept equals -4.2931.

Goodness of fit

Overall regression: right-tailed, F(1,8) = 2.874, p-value = 0.1285. Since p-value ≥ α (0.05), we accept H_0. The linear regression model, $\mathbf{Y = b_0 + b_1X + \varepsilon}$, doesn't provide a better fit than the model without the independent variable resulting in $\mathbf{Y = b_0 + \varepsilon}$. The slope ($b_1$): two-tailed, T(8)=1.6953, p-value = 0.1285. In the context of hypothesis testing in regression analysis, "two-tailed" refers to the type of test used to determine whether a parameter (such as the slope or y-intercept of a regression line) is significantly different from zero. A two-tailed test is used when we are interested in detecting deviations in both directions (both positive and negative) from the null hypothesis. Specifically, for a given significance level (α, often 0.05), a two-tailed test splits the alpha value into two tails at both ends of the distribution of the test statistic. The two-tailed test checks whether the slope is significantly different from zero. This means we are testing both the possibilities that the slope could be significantly greater than zero or significantly less than zero. In this case, the null hypothesis (H_0) is that the slope (b_1) is equal to zero (no relationship between q_c and E_{oed}), and the alternative hypothesis (H_1) is that the slope is not equal to zero (there is some relationship). For one predictor it is the same as the p-value for the overall model. The y-intercept (b_0): two-tailed, T(8) = 1.7212, p-value = 0.1235. Hence, b_0 is not significantly different from zero. It is still most likely recommended not to force b_0 to be zero. Similarly, for the y-intercept, the two-tailed test examines whether the intercept is significantly different from zero. Here, the null hypothesis is that the y-intercept (b_0) is zero, while the alternative hypothesis is that

the y-intercept is not zero. For both tests, if the p-value is less than the significance level (α = 0.05), we reject the null hypothesis, suggesting that the parameter is significantly different from zero. If the p-value is greater than α, we fail to reject the null hypothesis, indicating that there is not enough evidence to say the parameter is significantly different from zero.

Residual normality

The linear regression model assumes normality for residual errors. The Shapiro-Wilk p-value equals 0.9251. It is assumed that the data is normally distributed.

Figure 25 illustrates E_{oed} distribution and it is right-tailed.

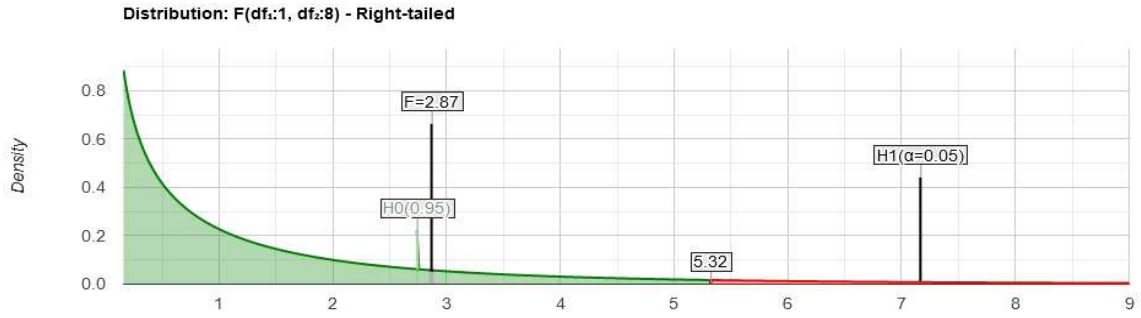

Figure 25: Distribution of Eoed

A right-tailed distribution, also known as positively skewed distribution, means that the majority of the data points cluster on the left side of the distribution, with the tail extending to the right. In other words, there are relatively few large values of E_{oed}, and these larger values create a "tail" that stretches out to the right. The distribution has a long tail on the right side, indicating that there are a few observations with much higher values than the rest. Most of the data values are concentrated on the lower end. In the given context, although the Shapiro-Wilk test p-value of 0.9251 suggests that the residuals are likely normally distributed (since $p > 0.05$), the right-tailed nature of the E_{oed} distribution itself might indicate that the original E_{oed} data has a positive skew. This discrepancy suggests that while the residuals (differences between observed and predicted values) of the regression model might be normally distributed, the raw E_{oed} data shows a tendency toward higher values.

Residual normality of E_{oed} is provided in Figure 26.

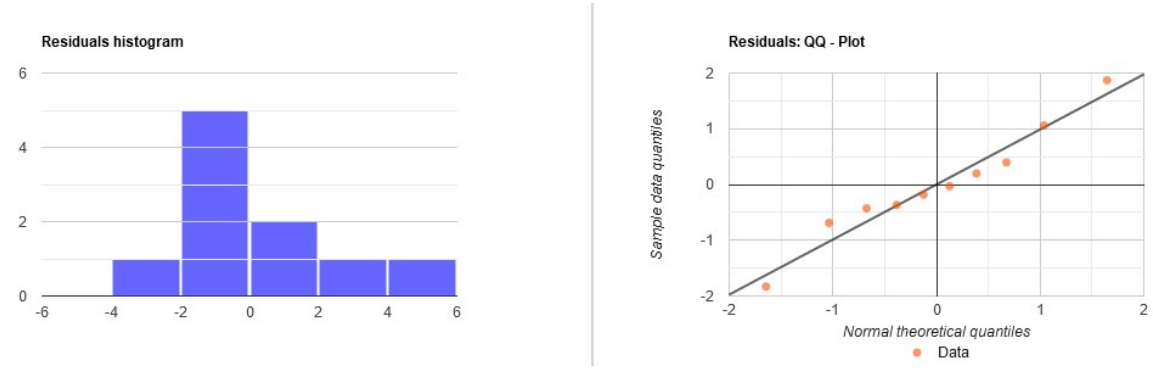

Figure 26: Residual Normality of Eoed

Table 13: Calculation of E_{oed} and q_c at different depths under 625 MPa stress

Stress (kPa)	E_{oed} (MPa)	Characteristic q_c value (MPa)	Depth, m
625	4.148	1.665	9.5-10.0
625	5.269	1.665	9.5-10.0
625	5.956	36.69	16.6-17.0
625	3.181	36.69	16.6-17.0
625	3.614	36.69	16.6-17.0
625	4.494	36.69	16.6-17.0
625	6.084	1.285	6.5-7.0
625	6.394	1.285	6.5-7.0
625	4.634	1.285	6.5-7.0
625	2.98	1.285	6.5-7.0

qc	Eoed	Ŷ (Predicted Y)	Residual
1.665	4.148	4.9145	-0.7665
1.665	5.269	4.9145	0.3545
36.69	5.956	4.3101	1.6459
36.69	3.181	4.3101	-1.1291
36.69	3.614	4.3101	-0.6961
36.69	4.494	4.3101	0.1839
1.285	6.084	4.9211	1.1629
1.285	6.394	4.9211	1.4729
1.285	4.634	4.9211	-0.2871
1.285	2.98	4.9211	-1.9411

Legend: Y-predicted values are E_{oed} predicted values

Figure 27: Regression calculation of oedometric modulus (E_{oed}) of soil mixtures without regressors of fine fraction (clay) and natural water content (w) under 625 kPa stress for all depths on EViews software

Regression line equation

$$\hat{Y} = 4.9433 - 0.01726X$$

Reporting linear regression in APA style

$R^2 = .066$, $F(1,8) = 0.57$, $p = .474$.$\beta = -.017$, $p = .474$, $\alpha = 4.94$, $p < .001$.

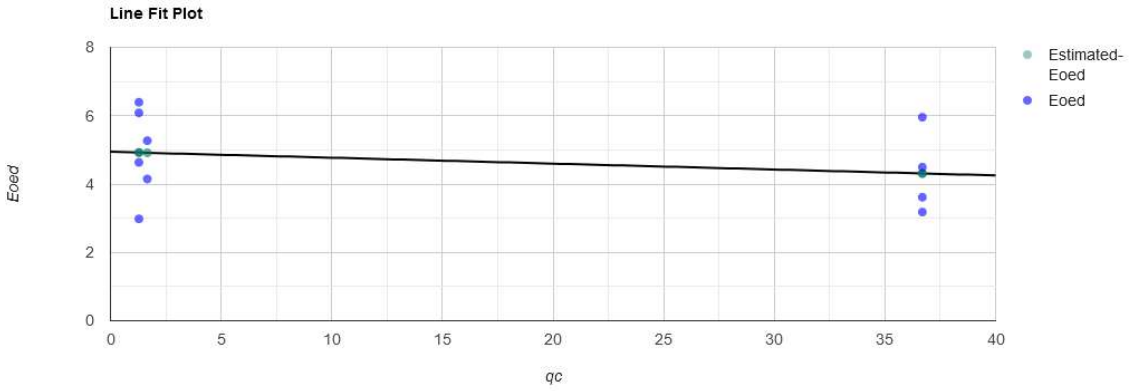

Figure 28: Line Fit Plot of Eoed estimated and Eoed determined

Figure 28 illustrates line fit plot of E_{oed} estimated and E_{oed} determined. Y-estimated values are E_{oed} estimated, it is given as light blue dots in the figure. Y values are E_{oed} determined values, they are shown as dark blue dots in the figure. Figure 29 provides prediction interval of E_{oed}. Black line shows regression line, blue line is 95% confidence interval and red line is 95% prediction interval.

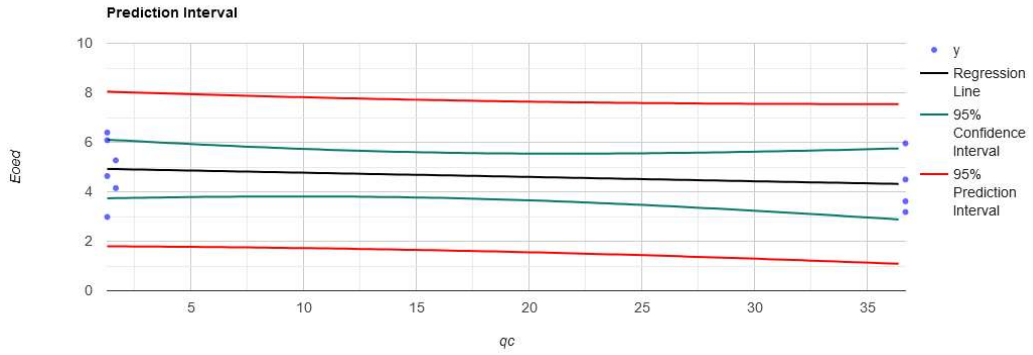

Figure 29: Prediction interval of E_{oed}

Figure 30 illustrated residual plot of E_{oed}.

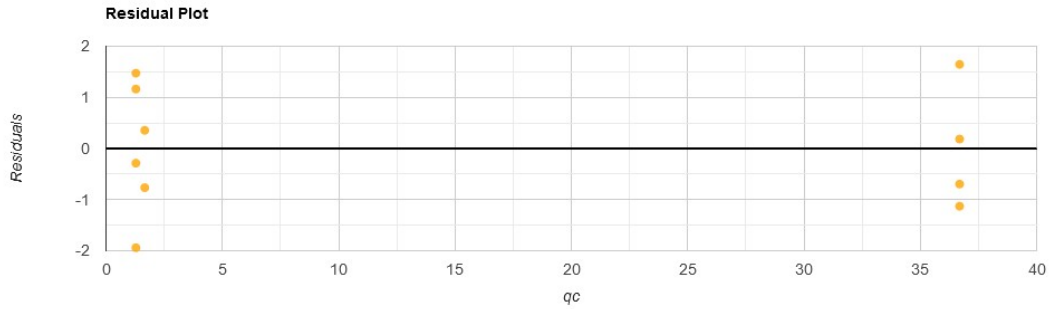

Figure 30: Residual plot of E_{oed}

Source	DF	Sum of Square	Mean Square	F Statistic (df_1,df_2)	P-value
Regression (between $\hat{y}_i$ and $\bar{y}$)	1	0.8895	0.8895	0.5653 (1,8)	0.4737
Residual (between y_i and $\hat{y}_i$)	8	12.5875	1.5734		
Total (between y_i and $\bar{y}$)	9	13.477	1.4974		

Figure 31: Regression analysis of E_{oed} in ANOVA

Figure 31 provides ANOVA regression calculation of E_{oed} by means of EViews software.

Explanation of ANOVA regression analysis is as follows:

E_{oed} and q_c relationship

R-Squared (R^2) equals **0.066.** This means that 6.6% of the variability of E_{oed} is explained by q_c. Correlation (R) equals **-0.2569**. This means that there is a **weak inverse relationship** between qc and Eoed. The Standard deviation of the residuals (S_{res}) equals **1.2544**. The slope: b_1=**-0.01726** CI[-0.07018, 0.03567] means that when you increase qc by 1, the value of Eoed decreases by 0.01726. The y-intercept: b_0=**4.9433** CI[3.7138, 6.1728] means that when qc equals 0, the prediction of Eoed's value is 4.9433. The x-intercept equals 286.468.

Goodness of fit

Overall regression: right-tailed, F(1,8) = 0.5653, p-value = 0.4737. Since p-value ≥ α (0.05), we accept H_0. The linear regression model, $\mathbf{Y = b_0 + b_1X + \varepsilon}$, doesn't provide a better fit than the model without the independent variable resulting in $\mathbf{Y = b_0 + \varepsilon}$. The slope ($b_1$): two-tailed, T(8)=-0.7519, p-value = 0.4737. For one predictor it is the same as the p-value for the overall model. The y-intercept (b_0): two-tailed, T(8) = 9.2715, p-value = 0.00001489. Hence, b_0 is significantly different from zero.

Residual normality

The linear regression model assumes normality for residual errors. The Shapiro-Wilk p-value equals 0.8364. It is assumed that the data is normally distributed.

Figure 32 illustrates E_{oed} distribution and it is right-tailed.

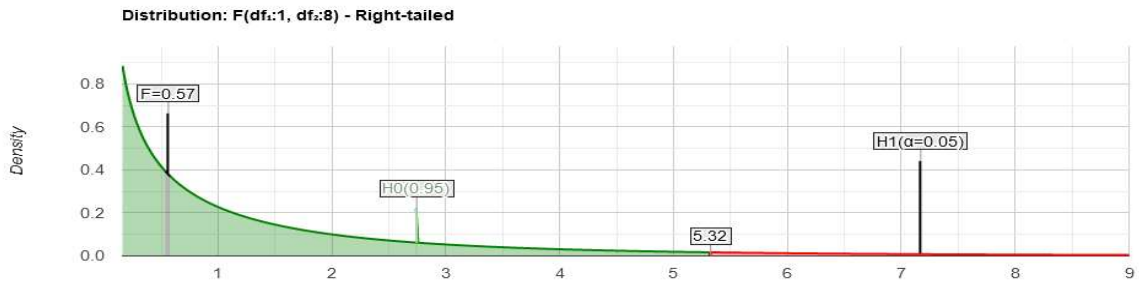

Figure 32: Distribution of Eoed

Residual normality of E_{oed} is provided in Figure 33.

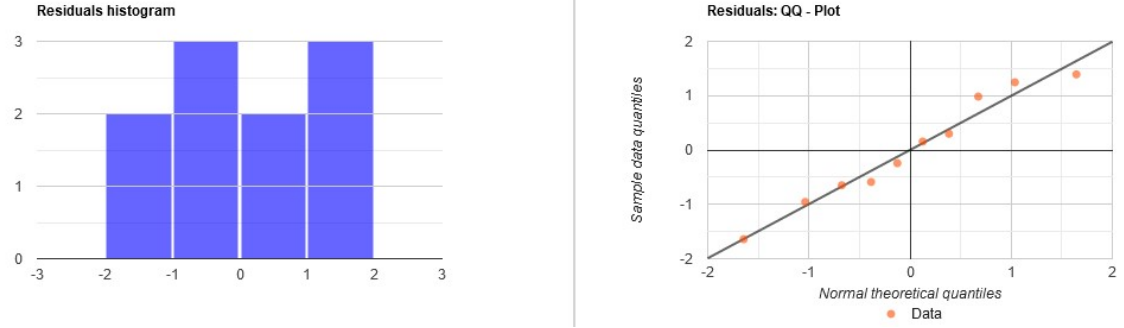

Figure 33: Residual Normality of Eoed

Afterwards, OCR values were calculated. The results of OCR calculations are provided in Table 14 and OCR illustration is provided in Figure 34. For preconsolidation stress, first we select point of maximum curvature, then from that point, draw a horizontal line. In our calculation it is orange line.

Then we draw a tangent line at that point. In this case, its orange line.

Then the two lines drawn (max. Curvature line and angle bisector line), we have to draw angle bisector of that line. In this case, this is green line.

Then we have to pick the last point of curve and draw linear line (blue line in this case).

This linear line touches at angle bisector line. We pick that point and the point is preconsolidation stress.

The illustration of this process is provided in Figure 34.

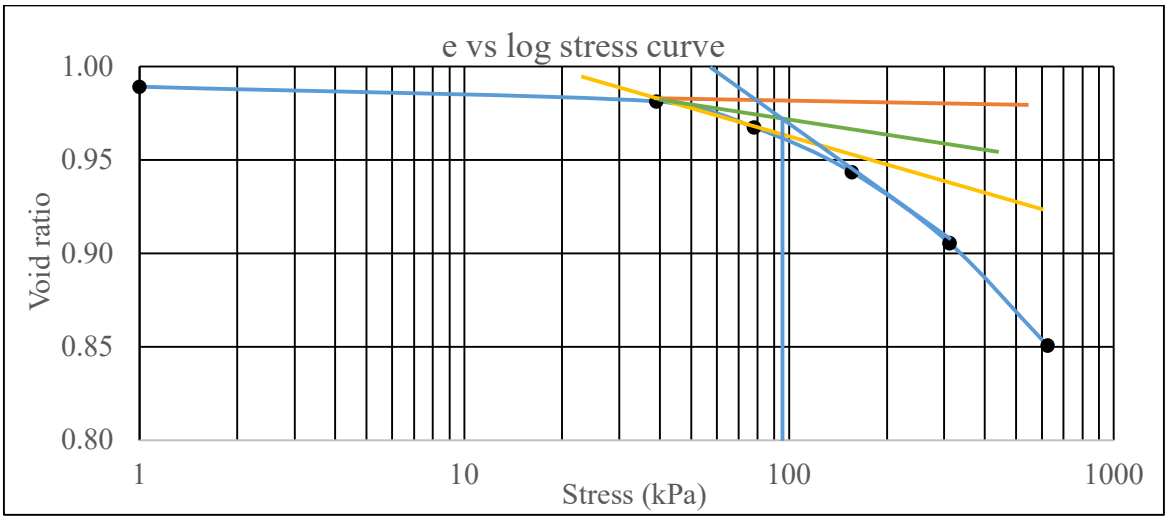

Figure 34: Illustration of pre-consolidation stress vs void ratio

Table 14: Results of OCR calculation

Depth of sample, m	OCR Result	Soil Name
6.5 – 7.0	2>1	Medium Plasticity Clay (ClL)
6.5 – 7.0	1,871794872 >1	Medium Plasticity Clay (ClL)
6.5 – 7.0	2,307692308 >1	Medium Plasticity Clay (ClL)
6.5 – 7.0	2,025641026 >1	Medium Plasticity Clay (ClL)
9.5 – 10.0	1,794871795 >1	Low Plasticity Clay (ClL)
9.5 – 10.0	1,538461538 >1	Low Plasticity Clay (ClL)
16.6 - 17.0	1,923076923 >1	Medium Plasticity Clay (ClL)
16.6 - 17.0	2,512820513 >1	Medium Plasticity Clay (ClL)
16.6 - 17.0	2,307692308 >1	Medium Plasticity Clay (ClL)
16.6 - 17.0	1,66666667 >1	Medium Plasticity Clay (ClL)

Statistical analysis of OCR calculation results is provided in Table 15.

Table 15: Descriptive statistics of OCR Results

Descriptive Statistics	Result
Minimum	min = 1.538461538
Maximum	max = 2.512820513
Range	R = 0.974358975
Size	n = 10
Sum	sum = 19.948718
Mean	$\bar{x}$ =1.9948718
Median	$\tilde{x}$ =1.9615384615
Mode	mode = 2.307692308
Standard Deviation	s = 0.305739291
Variance	s^2 = 0.09347658

Mid Range	MR = 2.025641025
Variance	5
Quartiles	Quartiles: Q_1 --> 1.794871795 Q_2 --> 1.9615384615 Q_3 --> 2.307692308
Interquartile Range	IQR = 0.512820513
Sum of Squares	SS = 0.841288625
Mean Absolute Deviation	MAD = 0.235897436
Root Mean Square	RMS = 2.0158478
Std Error of Mean	$SE_{\bar{x}}$ =0.0966832529
Skewness	γ_1 = 0.289348305
Kurtosis	β_2 = 3.6961034
Relative Standard Deviation	RSD = 15.3262626%

According to an article "OCR: Understanding Over Consolidation Ratio in Geotechnical Design" published in V Tech Journal of Geology of the UK[1], if overconcolidation ratio ranges less than 1, it means the soil type is normally consolidated soil. If the OCR value is greater than 1, it means the soil type is overconsolidated.

If OCR < 1, normally consolidated

If OCR > 1, over consolidated.

In our calculation, OCR was determined as greater than 1, so our soil samples are over-consolidated.

[1] OCR: Understanding Over Consolidation Ratio in Geotechnical Design, VJ Tech Limited, the UK, July 14, 2023, https://www.vjtech.co.uk/ocr-understanding-over-consolidation-ratio-in-geotechnical-design/ (Access date: 22.04.2024)

DISCUSSION AND LIMITATIONS

Correlation and regression analysis between q_c and E_{oed} at different stresses was performed by means of two different calculators (Geography Field Work Calculator and Stats Suite Regression Calculator) and EViews software.

Kelmė 19-1 at all stress levels: Despite the strong negative correlation indicated by the Rs (Spearman's Rank Correlation Coefficient) value in correlation between q_c and E_{oed} at different stresses for Kelmė 19-1, the high p-value (0.50) means that this relationship is not statistically significant. Given that the degrees of freedom are 0, the data set is extremely limited, which further undermines the confidence in these results. These results were concluded by Geography Field Work Calculator. As per Stats Suite Regression Calculator calculations for Kelme 19-1, the negative correlation coefficient (-0.5003) shows a moderate inverse relationship between q_c and E_{oed}. As qc increases, E_{oed} tends to decrease, but this relationship is not extremely strong. The linear regression analysis shows a moderate negative relationship between q_c and E_{oed}, with q_c explaining about a quarter of the variability in E_{oed}. While the model provides some insight into the relationship between these variables, the relatively low R^2 value suggests that there are other significant factors influencing E_{oed} that are not captured by q_c alone. As per null hypothesis, since the p-value (0.3907) is greater than the significance level ($\alpha = 0.05$), we fail to reject the null hypothesis. This means we do not have enough evidence to conclude that there is a statistically significant linear relationship between q_c and E_{oed}. The regression model does not show a statistically significant fit, indicating that q_c does not reliably predict E_{oed} in this data set. The large p-value and non-significant t-statistic suggest that the observed relationship between q_c and E_{oed} might be due to random chance rather than a true underlying linear relationship. The polynomial regression analysis indicates a quadratic relationship between q_c and E_{oed}, but the model does not provide a statistically significant improvement in explanatory power compared to a null model. The moderate R^2 value and the non-significant p-values for both the overall model and individual coefficients suggest that the relationship between q_c and E_{oed} for Kelmė 19-1 might be weak or influenced by other unaccounted factors.

Kelmė 19-2 at all stress levels: As per Geography Field Work Calculator, given the weak positive correlation (Rs=0.3) and the high p-value (greater than 0.50), we conclude that there is no statistically significant relationship between q_c and E_{oed} for Kelmė 19-2. The data suggests that any observed correlation might be due to random chance rather than an underlying linear relationship. Therefore, we accept the null hypothesis that there is no significant correlation between the two variables in this dataset. As per Stats Suite Regression Calculator, given the weak

positive correlation (r=0.1327), low explanatory power (R^2=0.0176), and the high p-value (0.8315), we conclude that there is no statistically significant relationship between q_c and E_{oed} for Kelmė 19-2. The data suggests that the observed correlation is likely due to random chance rather than a meaningful underlying relationship. Therefore, we accept the null hypothesis that there is no significant correlation between q_c and E_{oed} in this dataset. This analysis indicates that for Kelmė 19-2, qc does not provide a reliable predictor of E_{oed}. Further studies with a larger sample size and more variables might be necessary to explore potential relationships more thoroughly. The polynomial regression model for Kelmė 19-2 shows very limited explanatory power with an R^2 value of 0.0384. The model is not statistically significant as indicated by the F-statistic (0.04) and the associated p-value (0.9616). Additionally, none of the individual coefficients are statistically significant. Therefore, we conclude that the polynomial regression model does not provide a meaningful or significant explanation of the relationship between q_c and E_{oed} for Kelmė 19-2. The data suggests that there is no significant relationship between these variables, and the null hypothesis cannot be rejected.

Kelmė 37-2 at all stress levels: As per Geography Field Work Calculator, given the weak correlation and high p-value, we conclude that there is no statistically significant relationship between q_c and E_{oed} for Kelmė 37-2. The data does not support the existence of a meaningful correlation between these variables, and any observed association is likely due to random variability in the data. The analysis for Kelmė 37-2 according to Stats Suite Regression calculator shows that there is a weak positive correlation between q_c and E_{oed}. However, the relationship is not strong enough to be of practical significance. The low R^2 value indicates that the linear regression model does not adequately explain the variability in E_{oed}. Other factors likely contribute to the changes in E_{oed} that are not captured by qc alone. Therefore, while there is a slight tendency for E_{oed} to increase with q_c, the data does not support a robust or reliable predictive model for E_{oed} based on q_c. The null hypothesis that there is no correlation between q_c and E_{oed} cannot be rejected based on the given data. ANOVA regression model as a whole is not statistically significant at the conventional significance level of 0.05, as indicated by the low F-statistic and high associated p-value. Similarly, none of the individual coefficients are statistically significant. The polynomial regression model for Kelmė 37-2 does not provide a strong fit to the data.

The analysis of the multinomial logistic regression analysis between E_{oed} and q_c under 39 kPa stress (the lowest) indicates that the linear regression model is not statistically significant at the conventional significance level of 0.05, as the p-value for the F-statistic is 0.1285. The R-squared (R^2) value of 0.2643 indicates that approximately 26.4% of the variability in E_{oed} can be explained by q_c. The correlation coefficient (R) of 0.5141 suggests a moderate direct relationship

between q_c and E_{oed}. The slope (b_1) of 0.5457 indicates that for every unit increase in q_c, E_{oed} is expected to increase by 0.5457 units. The y-intercept (b_0) of 2.3427 suggests that when q_c equals 0, the predicted value of E_{oed} is 2.3427. The p-values for both the slope (b_1) and the y-intercept (b_0) are greater than 0.05, suggesting that neither parameter is significantly different from zero. The Shapiro-Wilk test for residual normality indicates a p-value of 0.9251, suggesting that the residuals are likely normally distributed. Overall, while there is a moderate direct relationship between q_c and E_{oed}, the linear regression model does not provide a significantly better fit than a model without the independent variable. The parameters of the regression model are not statistically significant, and the distribution of residuals appears to be normally distributed. Further analysis or alternative modeling approaches may be warranted to better understand the relationship between q_c and E_{oed} under 39 kPa stress.

The analysis of the multinomial logistic regression analysis between E_{oed} and q_c under 625 kPa stress (the highest) indicates that the linear regression model is not statistically significant at the conventional significance level of 0.05, as the p-value for the F-statistic is 0.4737. The p-value for the slope (b_1) is 0.4737, suggesting that the slope is not significantly different from zero. The y-intercept (b_0) has a p-value of 0.00001489, indicating that it is significantly different from zero. The Shapiro-Wilk test for residual normality indicates a p-value of 0.8364, suggesting that the residuals are likely normally distributed. The slope (b_1) of -0.01726 indicates that for every unit increase in q_c, E_{oed} decreases by 0.01726 units. The 95% confidence interval for b_1 is [0.07018, 0.03567], indicating that the true slope could be within this range. The y-intercept (b_0) of 4.9433 suggests that when q_c equals 0, the predicted value of E_{oed} is 4.9433. The 95% confidence interval for b_0 is [3.7138, 6.1728], indicating that the true intercept is significantly different from zero. The x-intercept is 286.468, which means the value of q_c where E_{oed} would be zero based on the regression equation. To sum up, the relationship between E_{oed} and q_c under 625 kPa stress is weak, as evidenced by the low R-squared value and the weak inverse correlation. The regression model does not significantly explain the variability in E_{oed}, and the slope parameter is not statistically significant. However, the y-intercept is significantly different from zero, indicating that the mean E_{oed} when q_c is zero is well estimated by the model. The residuals appear to be normally distributed, but the model overall does not provide a strong predictive capability for E_{oed} based on qc under this stress level. Further analysis or alternative models may be necessary to better capture the relationship.

Based on the calculations of OCR values, it was determined that the soil samples used in the tests were over-consolidated.

The findings contribute to a better understanding of the complex behavior of over-consolidated Pleistocene fine-grained till soils and provide valuable insights for geotechnical engineering applications. However, it is mandatory to acknowledge the limitations of laboratory tests in replicating real-world conditions, and further research may be needed for broader generalizations of the results.

Limitations: Due to thesis limited volume (limited to 60-65 pages of the main part excluding references and appendices), the analysis and correlations captured only most important part of the thesis. The study appears to have a small sample size (n), which limits the statistical power of the results. Small sample sizes can lead to less reliable estimates and reduced generalizability of the findings. The study is limited to specific conditions and locations (e.g., Kelmė sites). The findings may not be generalizable to other geographic regions or different soil conditions without further validation.

CONCLUSION

The study aimed to examine the relationship between q_c (cone tip resistance) and E_{oed} (deformation modulus) under different stress levels for various Kelmė soil samples. Despite using different analytical tools, including the Geography Field Work Calculator, Stats Suite Regression Calculator, and EViews software, the results consistently indicated weak and statistically insignificant relationships between q_c and E_{oed}.

Key findings are as follows:

Kelmė 19-1:

Despite a moderate negative correlation, the high p-values indicate no statistically significant linear or polynomial relationship between q_c and E_{oed}.

Kelmė 19-2:

Both correlation and regression analyses showed weak positive relationships with high p-values, indicating no significant relationship between q_c and E_{oed}.

Kelmė 37-2:

Analyses revealed weak correlations and low explanatory power, suggesting no significant relationship between qc and E_{oed}.

Stress-specific findings are as follows:

39 kPa Stress:

The linear regression model indicated a moderate direct relationship but was not statistically significant. Residuals were normally distributed, but the overall model fit was poor.

625 kPa Stress:

A weak inverse relationship was observed, but the regression model did not significantly explain the variability in E_{oed}. The y-intercept was significant, but the overall model was not predictive.

The study highlights the complexity of the relationship between q_c and E_{oed} in over-consolidated Pleistocene fine-grained till soils. Results indicate that qc alone is not a reliable predictor of E_{oed} under different stress levels. The findings underscore the limitations of laboratory tests in replicating real-world conditions and suggest that additional factors and more comprehensive models may be needed to better understand soil behavior. These insights are valuable for geotechnical engineering applications, emphasizing the need for further research and more robust modeling approaches to capture the intricate behaviors of soil properties.

REFERENCES

De Silva, H. S. U., Amarasekara, D. S. P., & Kurukulasuriya, L. C. (2022, September). Elastic and Shear Moduli of Over Consolidated Lime Stabilized Clayey Soil. *In 12th International Conference on Structural Engineering and Construction Management: Proceedings of the ICSECM 2021* (pp. 315-324). Singapore: Springer Nature Singapore.

Brilingas, A. (1988). Методика инженерно – геологических исследований для промышленного и гражданского строительства в районах расположения ледниковых отложений (на территории Литовской ССР). Диссертация на поиски ученой степи кандидата геолого-минералогических наук. (Metodika inzhenerno – geologicheskih izyskanij dlja promyshlennogo i grazhdanskogo stroitel‘stva v rajonah raspostranenija lednikovyh otlozhenij (na primere territorii Litovskoj SSR). Dissertacija na soiskanie uchenoj stepeni kandidata geologo–minearalogicheskih nauk.) PNIIIS. Moscow (in Russian)

Duncan J.M., Wright S.G., Brandon T.L. (2014) *Soil Strength and Slope Stability:* 2nd ed. New York: John Wiley and Sons, 317 p.

Fidelibus, M. D., Argentiero, I., Canora, F., Pellicani, R., Spilotro, G., & Vacca, G. (2018). Squeezed interstitial water and soil properties in Pleistocene Blue Clays under different natural environments. *Geosciences,* 8(3), 89.

Fithri E., Solin D.P. (2021) Correlation Between Cone Resistance Values and Cohesion Values in Cohesive Soils (Case Study in Gunung Anyar District), *E3S Web of Conferenc*es 328.

Gaur, A., & Sahay, A. (2017). Comparison of different soil models for excavation using retaining walls. *SSRG International Journal of Civil Engineering*, 4(3), 43-48.

Geotestus Report, 2023

Gribulis, D., Žaržojus, G., Gadeikis, S., Gadeikytė, S., & Urbaitis, D. (2019). Research of undrained shear strength of till fine soils (moraine). In The *13th international conference "Modern building materials, structures and techniques"*, 16–17 May, 2019, Vilnius, Lithuania (pp. 329-335). VGTU Press.

Habtemariam, B. G., Shirago, K. B., & Dirate, D. D. (2022). Effects of soil properties and slope angle on deformation and stability of cut slopes. Advances in Civil Engineering, 2022.

Håkansson, I., & Lipiec, J. (2000). A review of the usefulness of relative bulk density values in studies of soil structure and compaction. Soil and Tillage Research, 53(2), 71-85.

Huang, H., Huang, M., Ding, J. 2018. Calculation of Tangent Modulus of Soils under Different Stress Paths. Mathematical Problems in Engineering 2018 (6), 1–11.

Ibrahim, N. M., Rahim, N. L., Amat, R. C., Salehuddin, S., & Ariffin, N. A. (2012). Determination of plasticity index and compression index of soil at Perlis. Apcbee Procedia, 4, 94-98.

Jagodnik, V., & Marušić, D. (2023). Determination of the Atterberg limits using a Fall cone device on low plasticity silty sands. Rudarsko-geološko-naftni zbornik, 38(3), 133-145.

Jianqiao, L. I., Xiaodong, Z. H. A. N. G., Meng, Z. O. U., & Hao, L. I. (2012). Soil liquid limit and plastic limit treating system based on analytic method. Procedia Earth and Planetary Science, 5, 175-179.

Kwak, C., & Clayton-Matthews, A. (2002). Multinomial logistic regression. Nursing research, 51(6), 404-410.

Li, L., Zang, M., Zhang, R.-T., Lu, H.-J. 2022. Deformation and Strength Characteristics of Structured Clay under Different Stress Paths. Mathematical Problems in Engineering 2020 (9266206), 16 pp.

Lovisa, J., & Sivakugan, N. (2015). Tall oedometer testing: method to account for wall friction. International Journal of Geomechanics, 15(2), 04014045.

Lekstutytė, I., Urbaitis, D., Žaržojus, G., Skuodis, Š., & Gadeikis, S. (2023). Factors affecting the oedometric modulus of till soil. Baltica., 36(2), 190-205.

Malizia, P.J., Shakoor, A. 2018. Effect of water content and density on strength and deformation behavior of clay soils. Engineering Geology 24 (4), 125–131. https://doi.org/10.1016/j.enggeo.2018.07.028

Meyer, Z., & Olszewska, M. (2021). Methods Development for the Constrained Elastic Modulus Investigation of Organic Material in Natural Soil Conditions. Materials, 14(22), 6842.

Mohammed L. N., H. H. Titi, and A. Herath, (2000) "Evaluation of resilient modulus of subgrade soil by cone penetration test," Transportation Research Record, vol. 1652, pp. 236–245.

OCR: Understanding Over Consolidation Ratio in Geotechnical Design, VJ Tech Limited, the UK, July 14, 2023, https://www.vjtech.co.uk/ocr-understanding-over-consolidation-ratio-in-geotechnical-design/ (Access date: 22.04.2024)

Okewale, I. A., & Grobler, H. (2023, March). Investigation into Mechanical Behaviour of Tin Tailing Considering Incremental Loading Oedometer. In International Conference on Geosynthetics and Environmental Engineering (pp. 15-24). Singapore: Springer Nature Singapore.

Robertson, P. K. 2016. Cone Penetration Test (CPT)–Based Soil Behaviour Type (SBT) Classifcation System – an Update. Canadian Geotechnical Journal 53205(12). https://doi.org/10.1139/cgj-2016-0044

Sabarishri, K., Premalatha, K., & Arivazhagan, R. (2017). Influence of grain size and its distribution on the deformation Modulus and stress strain characteristics of sands. In Indian Geotechnical Conference GeoNEst 7 (1).

Sharma, L. K., Singh, R., Umrao, R. K., Sharma, K. M., & Singh, T. N. (2017). Evaluating the modulus of elasticity of soil using soft computing system. Engineering with Computers, 33, 497-507.

Sližytė, D., Medzvieckas, J. & Mackevičius, R. 2012. Pamatai ir pagrindai [Foundation and Base]. Technika, Vilnius, 248 pp. [in Lithuanian].

Tamošiūnas, T., Skuodis, Š., & Žaržojus, G. (2020). Overview of Quaternary sediments deformation modulus dependency on the testing methodology. *Baltica*, 33(2), 191–199.

Uyanık, G. K., & Güler, N. (2013). A study on multiple linear regression analysis. Procedia-Social and Behavioral Sciences, 106, 234-240.

Wang, J., Dai, M., Cai, Y., Guo, L., Du, Y., Wang, C., & Li, M. (2021). Influences of initial static shear stress on the cyclic behaviour of over consolidated soft marine clay. Ocean Engineering, 224, 108747.

Wei, H., Liu, H., Xiaoxiao, L., Zhao, T., Wu, Y., Shen, J., Yin, M. 2023. Effect of stress path on the mechanical properties of calcareous sand. Underground Space 9, 20–30.

Wu, S., Lok, T., Xu, Y., Wang, W., & Wu, B. (2021). Rate-dependent behavior of a saturated reconstituted clay under different over-consolidation ratios and sample variance. Acta Geotechnica, 16, 3425-3438.

Žaržojus, G., & Dundulis, K. (2010). Problems of correlation between dynamic probing test (DPSH) and cone penetration test (CPT) for cohesive soils of Lithuania. *The Baltic Journal of Road and Bridge Engineering,* 5(2), 69-75.

Žaržojus, G., Tamošiūnas, T., & Skuodis, Š. (2022). Indirect determination of soil Young's modulus in Lithuania using cone penetration test data. *The Baltic journal of road and brodge engineering*, 17(2), 1-24.

International Organization for Standardization. 2015. Geotechnical investigation and testing – Laboratory testing of soil – Part 2: Determination of bulk density (ISO 17892-2:2015). https://standards.iteh.ai/catalog/standards/sist/7a201656-a5cd-4a1a-91ecea69dc83ddb5/sist-en-iso-17892-2-2015

International Organization for Standardization. 2017. Geotechnical investigation and testing – Laboratory testing of soil –Part 5: Incremental loading oedometer test (ISO 17892-5:2017). https://www.iso.org/standard/55247.html

International Organization for Standardization. 2018. Geotechnical investigation and testing – Laboratory testing of soil – Part 12: Determination of Atterberg limits (ISO 17892-12:2018). https://www.iso.org/standard/72017.html

International Organization for Standardization. 2018.Geotechnical investigation and testing – Identifcation and classifcation of soil – Part 2: Principles for a classifcation (ISO 14688-2:2018). https://standards.iteh.ai/catalog/standards/cen/b8411dd6-1af7-4876-b5dd-9365aa50b5d2/en-iso-14688-2-2018.

SUMMARY

VILNIUS UNIVERSITY
FACULTY OF CHEMISTRY AND GEOSCIENCES

ANAR BAKHTIYAROV

RESEARCH OF OEDOMETRIC MODULUS AND ITS CORRELATION WITH CONE PENETRATION TEST RESULTS IN OVERCONSOLIDATED PLEISTOCENE FINE-GRAINED TILL SOILS

This thesis explores the relationship between the oedometric modulus (E_{oed}) and cone penetration resistance (q_c) in overconsolidated Pleistocene fine-grained till soils. The research aims to determine if q_c can reliably predict E_{oed} and understand the variability and complexity of these soil properties. The study employed a variety of analytical tools, including the Geography Field Work Calculator, Stats Suite Regression Calculator, and EViews software, to perform correlation and regression analyses on soil samples from multiple locations in Kelmė. The analyses were conducted under different stress levels to examine the relationship between q_c and $E_{oed.}$ For Kelmė 19-1, Geography Field Work Calculator showed a strong negative correlation with high p-values, indicating no statistical significance. Stats Suite Regression Calculator identified a moderate inverse relationship between q_c and E_{oed}, but the regression analysis did not show statistical significance (p-value = 0.3907). Polynomial regression also failed to provide significant explanatory power, suggesting that the relationship might be weak or influenced by other factors. For Kelmė 19-2, weak positive correlation (Rs = 0.3) with high p-values as per Geography Field Work Calculator, indicating no significant relationship. Stats Suite Regression Calculator showed a weak positive correlation (r = 0.1327) and low explanatory power (R2 = 0.0176), with high p-values, leading to the acceptance of the null hypothesis that there is no significant correlation. Polynomial regression confirmed very limited explanatory power and non-significant coefficients. For Kelmė 37-2, weak correlation and high p-values according to Geography Field Work Calculator, indicating no significant relationship. Stats Suite Regression Calculator found a weak positive correlation but low explanatory power (R2 = 0.0445), and the null hypothesis could not be rejected. Polynomial regression did not provide a strong fit to the data. The over-consolidated nature of the soils was confirmed by calculated OCR values.

APPENDICES

APPENDIX 1. CONSISTENCY TEST (FALLING CONE METHOD) ISO 17892-12:2004

Consistency Test of soil at 9.5 - 10.0 depth

Consistency Test (Falling Cone Method) ISO 17892-12:2004	
Object	Kelmė V7
Borehole No.	GR19-1
Depth of Sample (m)	9.5 - 10.0
Soil Name (According ISO 14688-2)	Low Plasticity Clay (ClL)

Trial #	1	2	3	4
Penetration (mm)	12.6	15.9	18	21.9
Can Mass (gm)	13.32	13.68	14.86	14.99
Can + Wet Soil Mass (gm)	30.65	35.19	36.63	34.89
Can + Dry Soil Mass (gm)	27.93	31.75	32.82	31.21
Weight of Dry Soil (gm)	14.61	18.07	17.96	16.22
Weight of Water (gm)	2.72	3.44	3.81	3.68
Moisture Content (%)	18.617	19.037	21.214	22.688

Cone Penetration of Moisture Dependence Graph of soil at depth 9.5 - 10.0

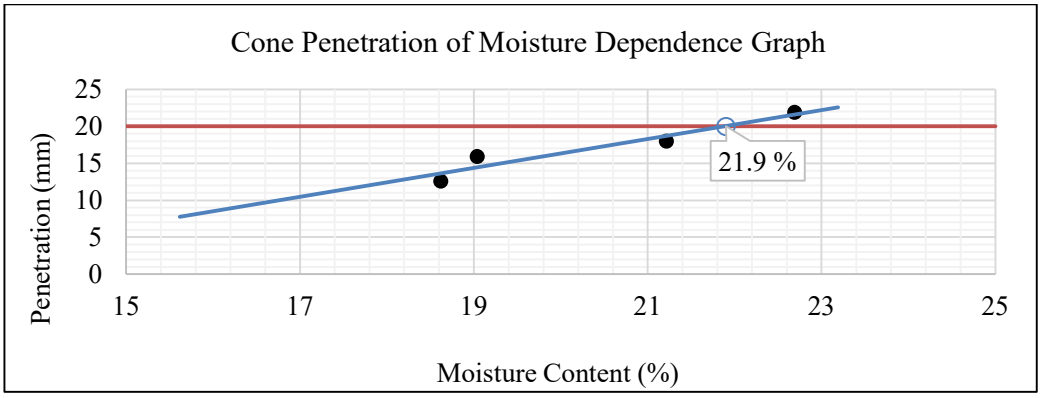

Consistency Test of soil at 16.6 - 17.0 depth

Consistency Test (Falling Cone Method) ISO 17892-12:2004	
Object	Kelmė V7
Borehole No.	GR19-1
Depth of Sample (m)	16.6 - 17.0
Soil Name (According ISO 14688-2)	Medium Plasticity Clay (ClM)

Trial #	1	2	3	4
Penetration (mm)	11.8	14.3	18.1	21.7

Can Mass (gm)	15.01	14.19	15.02	13.52
Can + Wet Soil Mass (gm)	32.23	33.07	32.75	34.81
Can + Dry Soil Mass (gm)	27.85	27.89	27.86	28.54
Weight of Dry Soil (gm)	12.84	13.7	12.84	15.02
Weight of Water (gm)	4.38	5.18	4.89	6.27
Moisture Content (%)	34.112	37.810	38.084	41.744

Cone Penetration of Moisture Dependence Graph of soil at depth 16.6 - 17.0

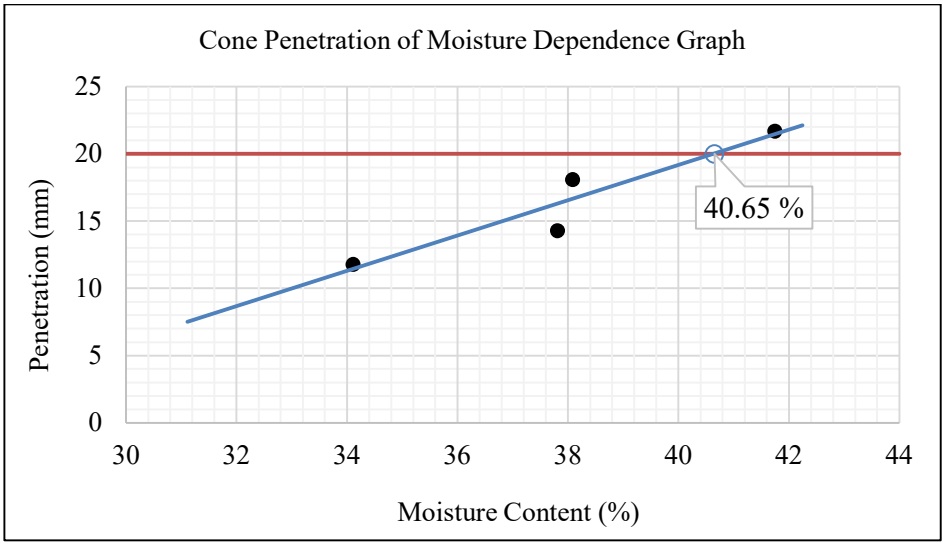

Consistency Test of soil at 6.5 - 7.0 depth

Consistency Test (Falling Cone Method) ISO 17892-12:2004	
Object	Kelmė V7
Borehole No.	37 2
Depth of Sample (m)	6.5 - 7.0
Soil Name (According ISO 14688-2)	Medium Plasticity Clay (CIM)

Trial #	1	2	3	4
Penetration (mm)	12.25	14.5	17.6	20
Can Mass (gm)	13.49	12.96	14.8	15
Can + Wet Soil Mass (gm)	28.44	24.45	35.13	29.20
Can + Dry Soil Mass (gm)	26.11	22.57	31.61	26.70

Weight of Dry Soil (gm)	12.62	9.61	16.81	11.70
Weight of Water (gm)	2.33	1.88	3.52	2.50
Moisture Content (%)	18.463	19.563	20.940	21.368

Cone Penetration of Moisture Dependence Graph of soil at depth 6.5 - 7.0

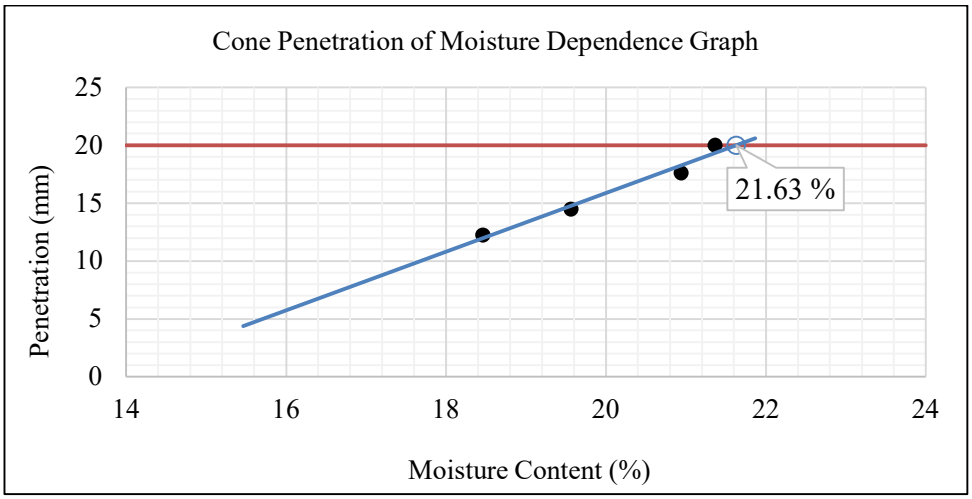

APPENDIX 2. BULK DENSITY 17892-2:2014 & WATER CONTENT ISO 17892-1:2014 RESULTS

Borehole No.	Specimen Depth (m)	Soil Description	Bulk Density, ρ (Mg/m^3)	Water Content, w (%)
GR19-1	9.5 - 10.0	CIL	2,03	12.53
GR19-1	9.5 - 10.0	CIL	2,28	12.55
GR19-1	9.5 - 10.0	CIL	2,25	12.68
GR19-1	9.5 - 10.0	CIL	2,04	13.78
GR19-2	16.6 - 17.0	CIM	2,02	17.40
GR19-2	16.6 - 17.0	CIM	2,20	18.76
GR19-2	16.6 - 17.0	CIM	2,22	17.94
GR19-2	16.6 - 17.0	CIM	2,08	18.37
37 2	6.5 - 7.0	CIM	2,03	10.46
37 2	6.5 - 7.0	CIM	2,29	11.13
37 2	6.5 - 7.0	CIM	2,29	10.95
37 2	6.5 - 7.0	CIM	2,08	10.82

APPENDIX 3. THE RESULTS OF THE OEDOMETER TESTS AT DEPTH OF 9.5 TO 10 M OF BOREHOLE GR19-1, AT DEPTH OF 16.6 TO 17 M OF BOREHOLE GR19-2 AND AT DEPTH OF 6.5 TO 7 M OF BOREHOLE GR37-2 AT DIFFERENT MOISTURE CONTENTS AND BULK DENSITY

Results of Incremental loading oedometer test for GR19-1 at w =12.53%

Borehole No.		GR19-1	**Depth of Sample (m)**	9.5-10.0			
Soil Name (According ISO 14668-2)			Low Plasticity Clay (ClL)				
Moisture Content, w	12,53%	**Bulk density ρ**	1.56 mg/m3				
Stress, σ (kPa)	Void ratio, e	Strain, ε (%)	Oedometer, Modulus Eoed (MPa)	Coefficient of Volume Compressibility, mv (MPa)	Compression Index, Cc	t90 (min)	Coefficient of Consolidation, cv (mm2/min)
39	0,917	1,2	3,25	0,308		-	-
78	0,901	2,04	1,912	0,218	0,054	53,29	1,591
156	0,876	3,33	2,342	0,169	0,083	23,717	3,576
312	0,836	5,385	2,897	0,136	0,132	14,977	5,662
625	0,794	7,545	4,148	0,073	0,139	11,903	7,125

Results of Incremental loading oedometer test for GR19-1 at w =13.68%

Borehole No.		GR19-1	**Depth of Sample (m)**	9.5-10.0			
Soil Name (According ISO 14668-2)			Low Plasticity Clay (ClL)				
Moisture Content, w	13,68%	**Bulk density ρ**	1.57 mg/m3				
Stress, σ (kPa)	Void ratio, e	Strain, ε (%)	Oedometer, Modulus Eoed (MPa)	Coefficient of Volume Compressibility, mv (MPa)	Compression Index, Cc	t90 (min)	Coefficient of Consolidation, cv (mm2/min)
39	0,918	1,55	2,516	0,397		29,703	2,855
78	0,903	2,345	1,663	0,207	0,051	21,16	4,008
156	0,883	3,345	2,332	0,131	0,065	7,952	10,663
312	0,858	4,62	3,377	0,085	0,083	9	9,422
625	0,833	5,94	5,269	0,044	0,085	13,69	6,194

Results of Incremental loading oedometer test for GR19-2 at w =17.40%

Borehole No.		GR19-2	**Depth of Sample (m)**		16.6-17.0		
Soil Name (According ISO 14668-2)			Medium Plasticity Clay (ClM)				
Moisture Content, w	17,40%	**Bulk density ρ**	1.55 mg/m3				
Stress, σ (kPa)	Void ratio, e	Strain, ε (%)	Oedometer, Modulus Eoed (MPa)	Coefficient of Volume Compressibility, mv (MPa)	Compression Index, Cc	t90 (min)	Coefficient of Consolidation, cv (mm2/min)
39	1,019	0,585	6,667	0,15		4	21,2
78	1,007	1,16	3,362	0,148	0,039	15,21	5,575
156	0,975	2,775	2,811	0,209	0,109	12,25	6,922
312	0,956	3,705	4,211	0,061	0,063	26,523	3,197
625	0,924	5,255	5,956	0,051	0,104	45,563	1,861

Results of Incremental loading oedometer test for GR19-2 at w =18.37%

Borehole No.		GR19-2	**Depth of Sample (m)**		16.6-17.0		
Soil Name (According ISO 14668-2)			Medium Plasticity Clay (ClM)				
Moisture Content, w	18,37%	**Bulk density ρ**	1.60 mg/m3				
Stress, σ (kPa)	Void ratio, e	Strain, ε (%)	Oedometer, Modulus Eoed (MPa)	Coefficient of Volume Compressibility, mv (MPa)	Compression Index, Cc	t90 (min)	Coefficient of Consolidation, cv (mm2/min)
39	0,981	0,395	9,873	0,101		5,063	16,751
78	0,968	1,09	3,578	0,179	0,046	14,977	5,562
156	0,943	2,3	3,391	0,157	0,08	16,81	5,045
312	0,905	4,21	3,705	0,125	0,126	33,64	2,521
625	0,851	6,965	4,494	0,092	0,182	38,813	2,185

Results of Incremental loading oedometer test for GR37-2 at w =10.46%

Borehole No.		GR37-2	**Depth of Sample (m)**	6.5-7.0			
Soil Name (According ISO 14668-2)			Medium Plasticity Clay (ClM)				
Moisture Content, w	10,46%	**Bulk density ρ**	1.56 mg/m3				
Stress, σ (kPa)	Void ratio, e	Strain, ε (%)	Oedometer, Modulus Eoed (MPa)	Coefficient of Volume Compressibility, mv (MPa)	Compression Index, Cc	t90 (min)	Coefficient of Consolidation, cv (mm2/min)
39	0,886	0,7	5,571	0,179		42,25	2,007
78	0,874	1,355	2,878	0,169	0,041	62,41	1,359
156	0,854	2,4	3,25	0,136	0,066	19,36	4,38
312	0,829	3,735	4,177	0,088	0,084	16,403	5,17
625	0,802	5,145	6,084	0,047	0,089	14,823	5,721

Results of Incremental loading oedometer test for GR37-2 at w =10.82%

Borehole No.		GR37-2	**Depth of Sample (m)**	6.5-7.0			
Soil Name (According ISO 14668-2)			Medium Plasticity Clay (ClM)				
Moisture Content, w	10,82%	**Bulk density ρ**	1.60 mg/m3				
Stress, σ (kPa)	Void ratio, e	Strain, ε (%)	Oedometer, Modulus Eoed (MPa)	Coefficient of Volume Compressibility, mv (MPa)	Compression Index, Cc	t90 (min)	Coefficient of Consolidation, cv (mm2/min)
39	0,808	2,205	1,769	0,565		22,563	3,758
78	0,787	3,325	1,173	0,294	0,069	16,974	4,996
156	0,752	5,225	1,493	0,252	0,117	12,96	6,543
312	0,708	7,61	2,05	0,161	0,146	8,123	10,44
625	0,654	10,505	2,98	0,1	0,177	17,724	4,784

APPENDIX 4. THE RESULTS OF GEOTESTUS REPORT ON CROSS-SECTIONS ANALYSIS

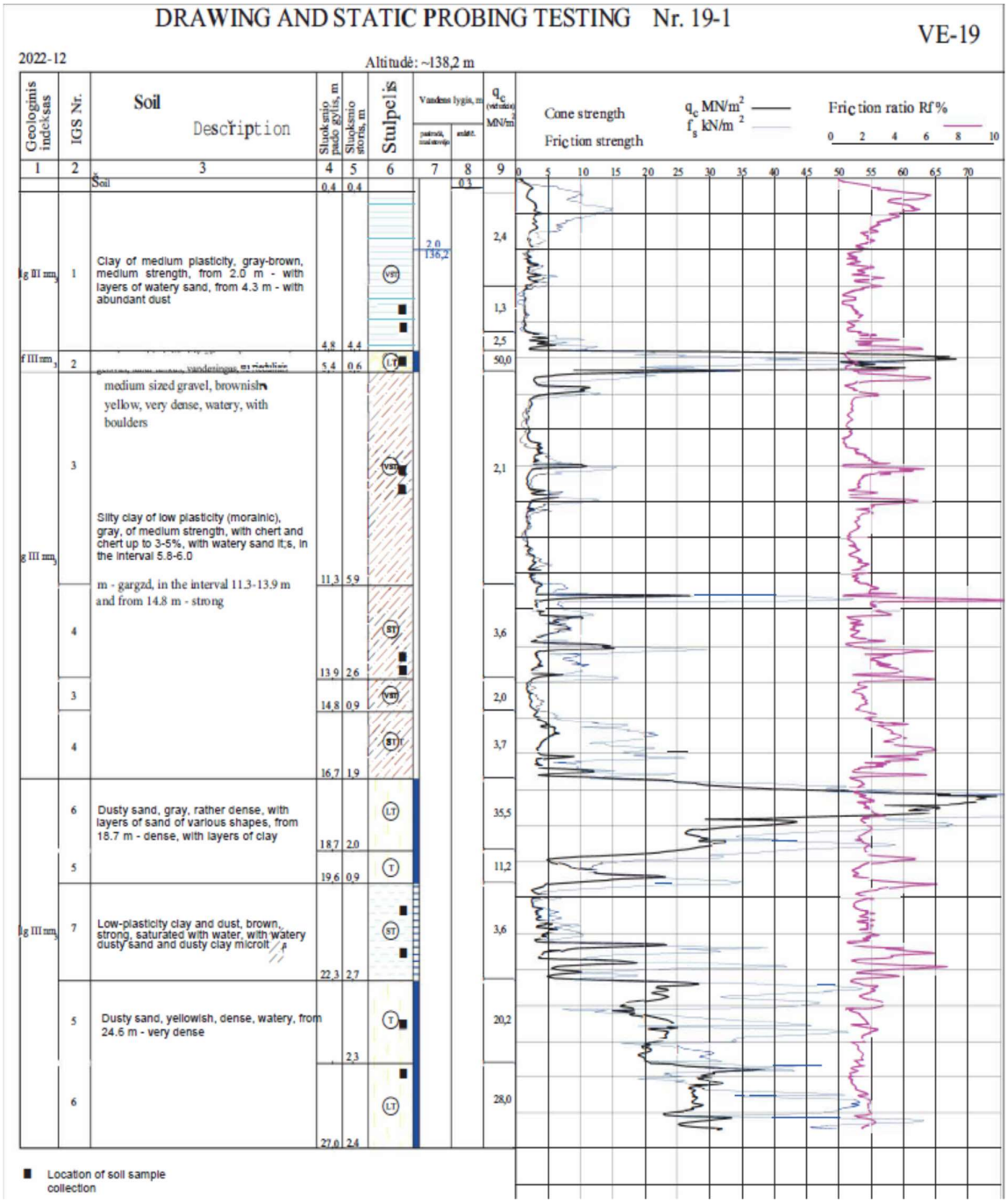

Layers of Kelmė 19-1 based on CPT (Source: Geotestus Report)

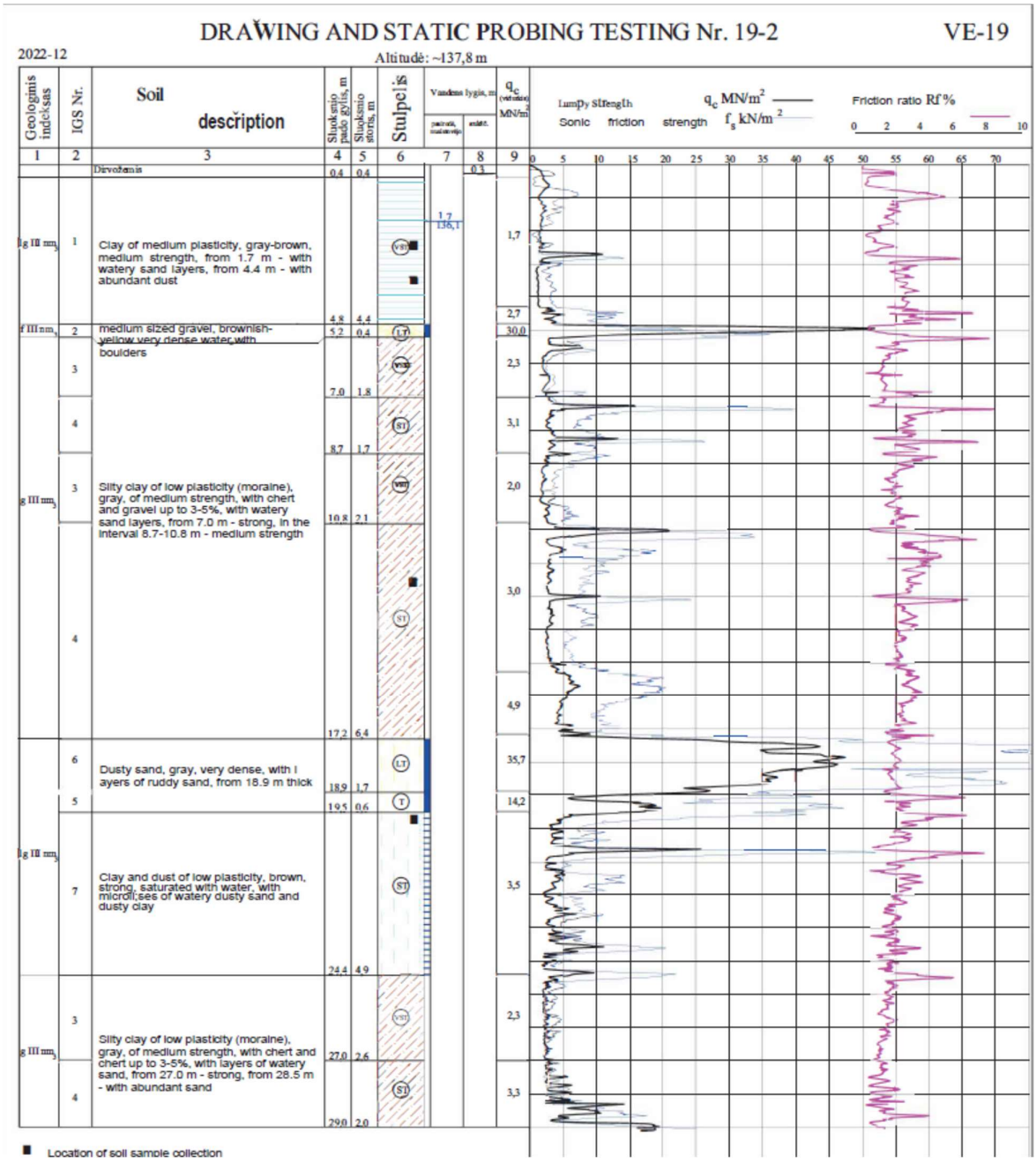

Layers of Kelmė 19-2 based on CPT (Source: Geotestus Report)

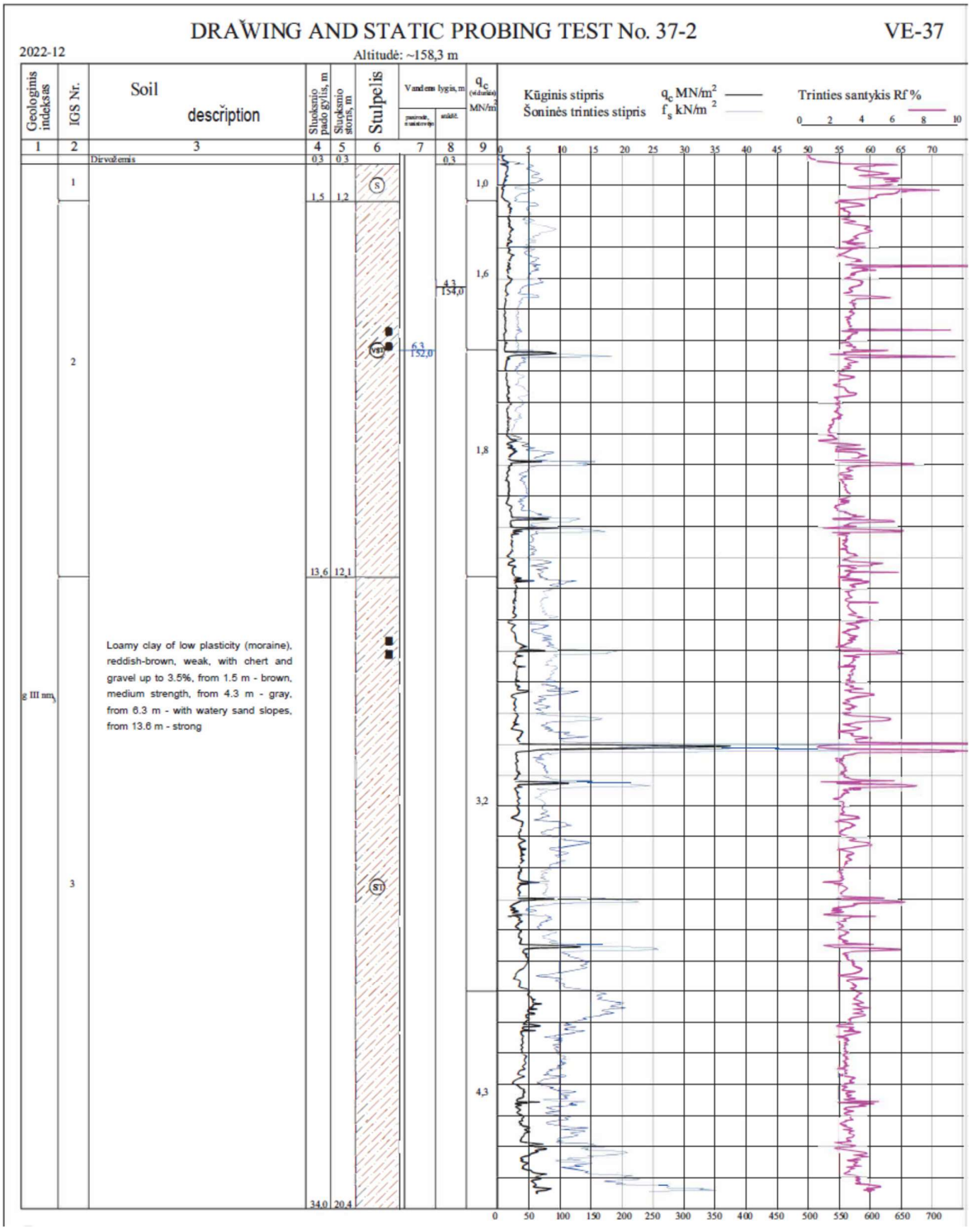

Layers of Kelmė 37 -2 based on CPT (Source: Geotestus Report)

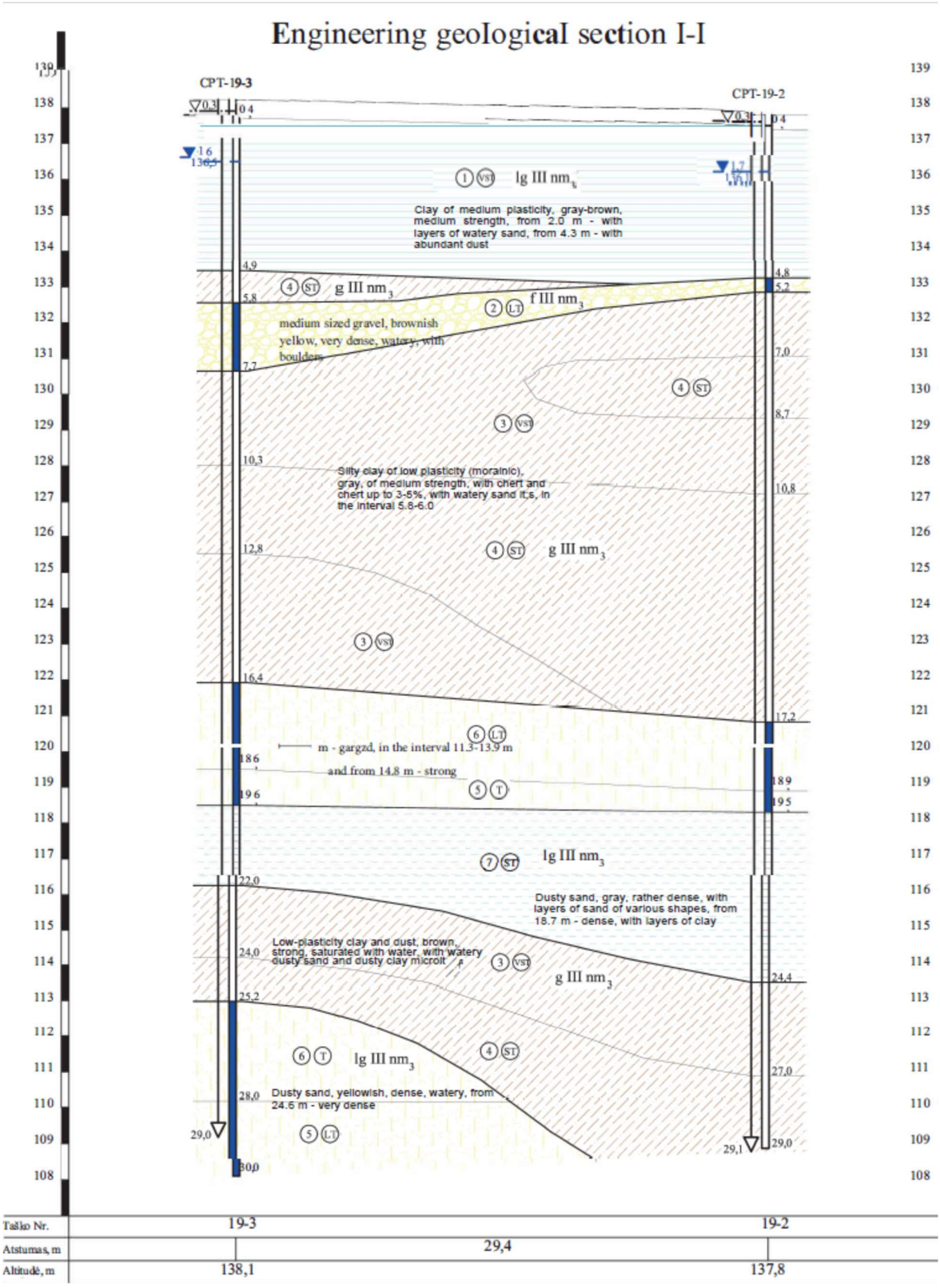

Engineering Geological Section I-I Kelmė 19 (Source: Geotestus Report, 2023)

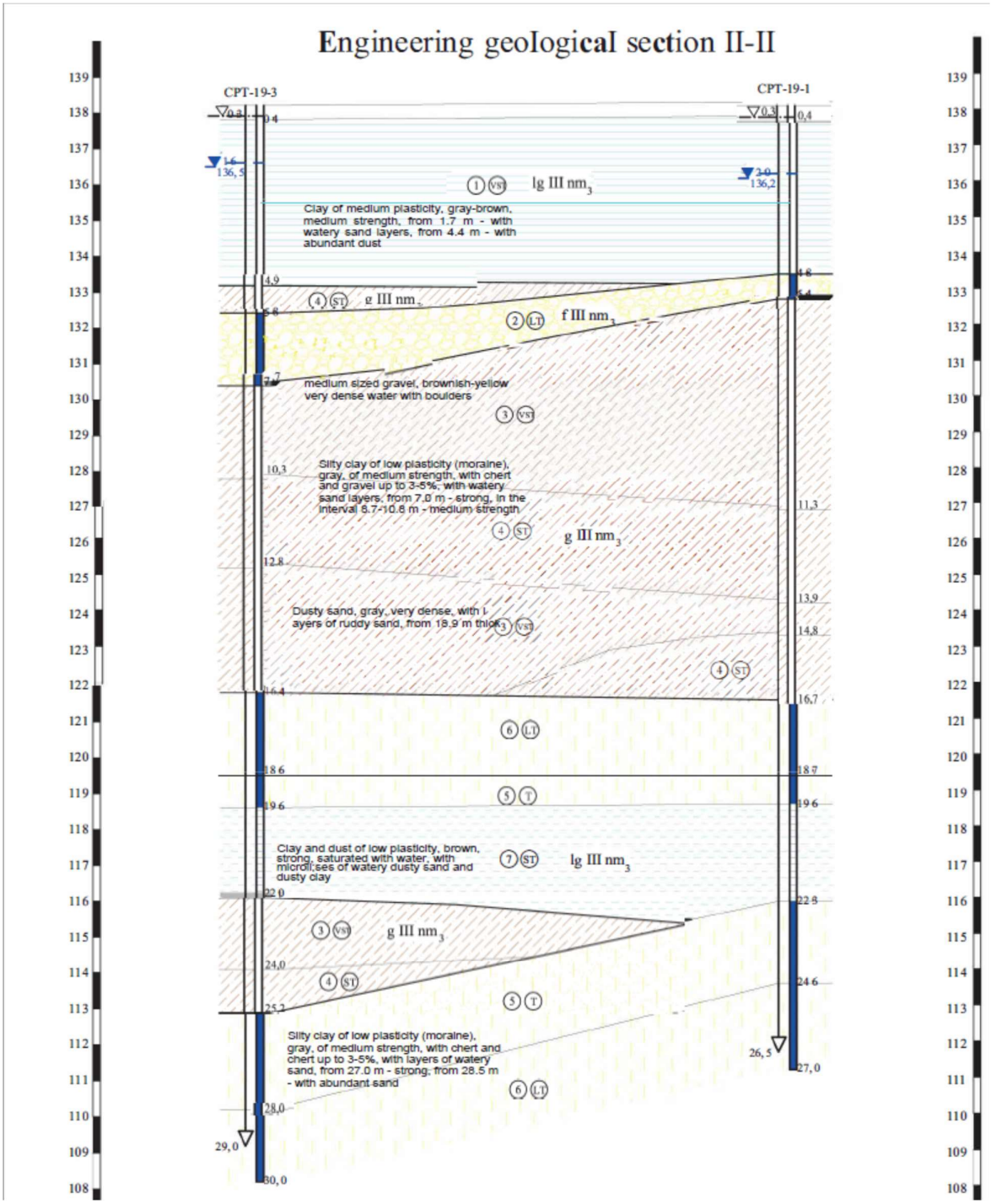

Engineering Geological Section II-II Kelmė 19 (Source: Geotestus Report, 2023)

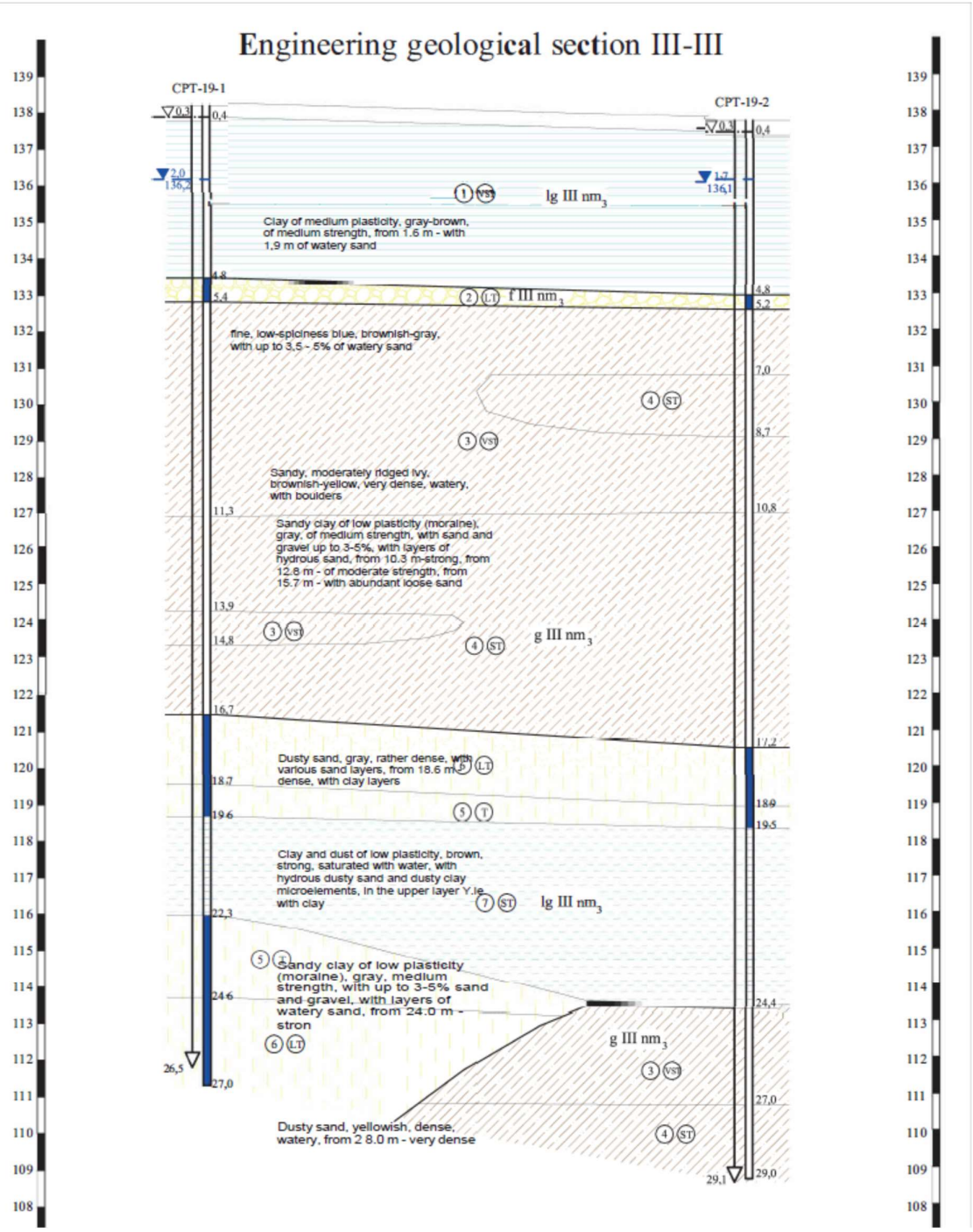

Engineering Geological Section III-III Kelmė 19 (Source: Geotestus Report, 2023)

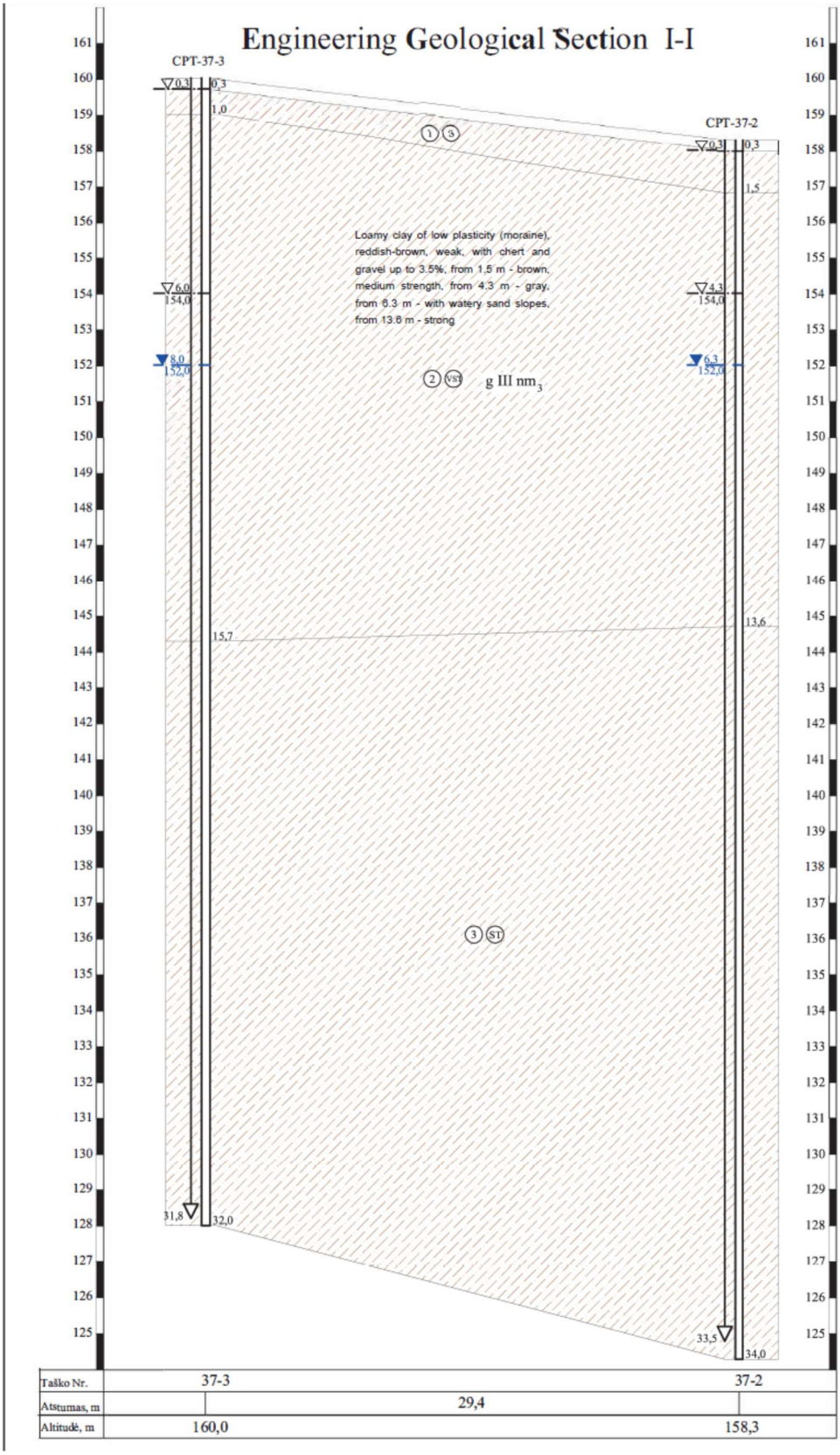

Engineering Geological Section I-I Kelmė 37 (Source: Geotestus Report, 2023)

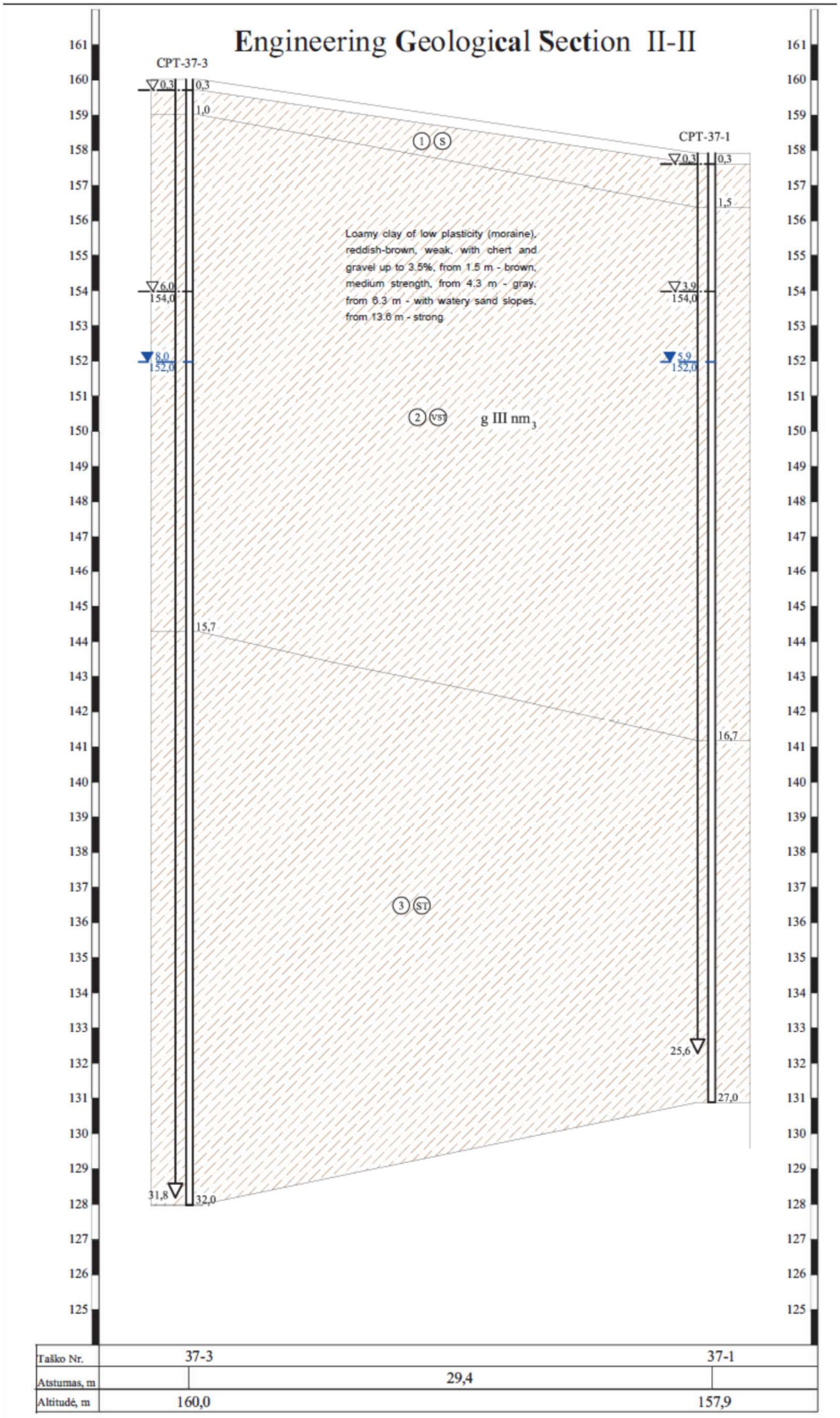

Engineering Geological Section II-II Kelmė 37 (Source: Geotestus Report, 2023)

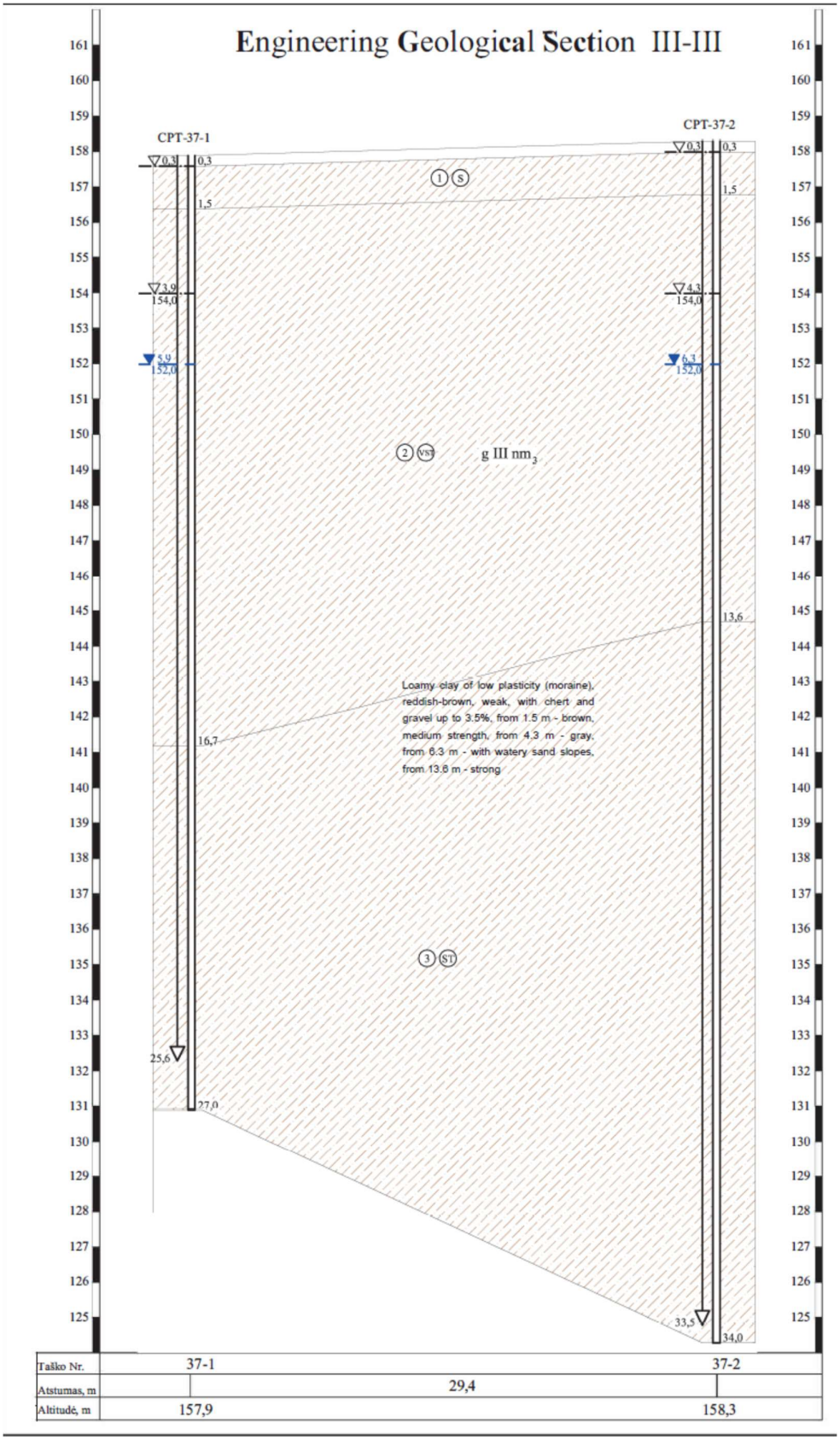

Engineering Geological Section III-III Kelmė 37 (Source: Geotestus Report, 2023)